Applied Mathematical Modelling 129 (2024) 250–274

Contents lists available at ScienceDirect

Applied Mathematical Modelling

journal homepage: www.elsevier.com/locate/apm

Mass moments of functionally graded 2D domains and axisymmetric solids

Davide Pellecchia [a,*], Nicolò Vaiana [a], Salvatore Sessa [a], Anna Castellano [b]

[a] Department of Structures for Engineering and Architecture, University of Naples Federico II, via Claudio 21, 80125 Naples, Italy
[b] Department of Architecture, Construction and Design, Politecnico di Bari, via Orabona 4, 70125 Bari, Italy

ARTICLE INFO

Keywords:
Mass moments
Functionally graded beams
Functionally graded axisymmetric solids
Additive manufacturing
Closed-form solutions

ABSTRACT

We present a general methodology to evaluate the mass moments of two-dimensional domains and axisymmetric solids made of functionally graded materials. The approach developed in the paper is based on the sequence of two steps. First, the original domain integrals are converted to integrals extended to the relevant boundary by exploiting Gauss theorem. Second, for domains having a polygonal or circular shape, the boundary integrals are evaluated analytically by providing algebraic expressions that depend upon the parameters defining the density distribution, the position vectors of the vertices of the polygonal domain or the initial and ending points of an arbitrary circular sector, respectively. While the first step refers to moments of arbitrary order, the second step is limited to the most useful quantities for engineering applications, i.e. generalised mass, static moment and inertia tensor. The formulas derived in the paper are validated by means of examples retrieved from the specialised literature for which analytical results are available or have been specifically derived by the authors. Finally, in order to ascertain the computational savings entailed by the use of the proposed analytical formulas with respect to numerical techniques, the mass moments of a longitudinal section of a human femure, made of a functionally graded material and characterised by a linear density distribution, have been computed.

1. Introduction

Functionally Graded Materials (FGMs) are materials obtained by combining different mechanical properties that exhibit special functionalities. For this reason, they have been commonly applied in the engineering sciences in the last thirty years, such as aerospace, civil, construction and electronics.

The possibility of designing and manufacturing composite materials in a quite arbitrary way has more recently allowed for the use of FGM in orthopaedic implants and bone studies [1], graphene platelets [2], and so on. Furthermore, FGMs have been instrumental in analysing the free vibration and buckling behaviour of Euler-Bernoulli columns [3] and plates [4].

In this respect, the evaluation of geometric properties, such as mass, static moment, and inertia tensor (also called moments of order 0, 1, and 2), is crucial for analysing mechanical systems and designing two- (2D) and three-dimensional (3D) engineering components [5,6]; for instance, the determination of the centre of gravity plays a paramount role in statics [7,8] and dynamics [9,10], both for 2D and 3D applications contexts.

* Corresponding author.
E-mail address: davide.pellecchia@unina.it (D. Pellecchia).

https://doi.org/10.1016/j.apm.2024.01.028
Received 15 September 2023; Received in revised form 9 January 2024; Accepted 16 January 2024

Available online 19 January 2024
0307-904X/© 2024 The Author(s). Published by Elsevier Inc. This is an open access article under the CC BY-NC-ND license (http://creativecommons.org/licenses/by-nc-nd/4.0/).

Let Ω be a domain having a mass density ϱ and P an arbitrary point of Ω with coordinates x, y in a Cartesian reference frame $\{O, \mathbf{e}_1, \mathbf{e}_2\}$ where O is a generic point and $\mathbf{e}_1, \mathbf{e}_2$ are orthogonal unit vectors. Denoting by $\boldsymbol{\rho} = x\,\mathbf{e}_1 + y\,\mathbf{e}_2$ the position vector of P, the mass moments of Ω of order k, k being a non-negative integer, are defined by

$$\mathbf{J}_{2\Omega}^{(k),\varrho} = \int_{\Omega} \varrho(\boldsymbol{\rho})\,[\otimes\boldsymbol{\rho},\ k]\,\mathrm{d}A, \tag{1}$$

where the symbol $[\otimes\boldsymbol{\rho},\ k]$ stands for

$$[\otimes\boldsymbol{\rho},\ k] = \begin{cases} 1 & \text{if } k = 0, \\ \boldsymbol{\rho} & \text{if } k = 1, \\ \boldsymbol{\rho} \otimes \boldsymbol{\rho} & \text{if } k = 2, \\ \cdots\cdots\cdots\cdots & \cdots\cdots \\ \underbrace{\boldsymbol{\rho} \otimes \boldsymbol{\rho} \otimes \cdots \otimes \boldsymbol{\rho}}_{k \text{ times}} & \text{if } k > 2. \end{cases}$$

Analogously, we shall denote by

$$\mathbf{J}_{\mathrm{ax}\Omega}^{(k),\varrho} = 2\,\pi \int_{\Omega} \varrho(\boldsymbol{\rho})\,[\otimes\boldsymbol{\rho},\ k]\,(\boldsymbol{\rho} \cdot \mathbf{b})\,\mathrm{d}A, \tag{2}$$

the k-th mass moment of axisymmetric solids in which the direction orthogonal to the axis of revolution is defined by the unit vector $\mathbf{b}$. Explicit formulas for the analytical computation of (1) and (2) will be presented only for $k = 0$, $k = 1$ and $k = 2$ since they represent the most frequent cases in the applications.

Despite their importance, the evaluation of these properties for domains having arbitrary shape is not always a trivial task, even for homogeneous 2D domains, i.e. domains characterised by a constant density. In fact, the evaluation of the geometric properties is usually presented in the literature in terms of domain integrals, which requires an analytical procedure that, apart from simple geometrical shapes such as rectangle, circle, and so on, can seldom be pursued.

The approach exploited till now to compute generalised mass moments, i.e. mass moments of solids having an inhomogeneous density, has been the use of numerical methods such as the Monte Carlo technique or the finite element method. In the last case the original domain is decomposed into standard elemental regions like triangles or quadrangles and Gauss integration is used.

More recently, Ochiai has presented in [11,12] a procedure for computing the mass moments of inhomogeneous domains based on the boundary element method [13], wherein the original domain integrals have been rephrased as boundary integral equations discretised by constant or linear elements; this required the solution of a linear system of equations for computing the interpolation parameters.

A much more effective approach for computing mass moments is based on the transformation of the original domain integral into a boundary integral by means of Gauss theorem although the relevant details are rarely presented in books, a remarkable exception being [14], and are limited to papers [15] or web pages. Subsequently, mass moments expressed in terms of boundary integrals are evaluated analytically for the domains of greater interest in the applications such as the circular or polygonal ones. Of particular importance are these last ones since any 2D domain can be approximated by a polygonal shape.

The same approach has been successfully exploited in several engineering applications in which complex domain integrals need to be efficiently computed. We mention, among others, the elastic-plastic response of concrete sections [16], the ultimate limit analysis of reinforced concrete sections [17–19], the evaluation of displacement, strain and stress fields in elastic half-spaces loaded on their surface by thermal actions [20] or by arbitrary distributions of surface pressures [21–23]. Further applications refer to bifurcation analysis of isotropic elastic solids [24–27], to geodesy [28,29] and to domains with small voids as in the case of porous materials [30, 31]. More recently Gauss theorem has been applied to solve the Eshelby inclusion problem both for two-dimensional [32] and three-dimensional [33] elastic domains.

Motivated by the previous considerations, we present an approach, based on Gauss theorem, to analytically compute the mass moments of functionally graded 2D domains and axisymmetric solids having arbitrary shape. For polygons and circular sectors, this leads to analytical formulas, thus completely avoiding the need to discretise the domain, as in the finite element method, or solve a linear system of equations, as in [11,12]. Specifically, the formulas derived in the paper depend upon the parameters defining the non-constant mass density and geometric quantities. These are the coordinates of the vertices for polygonal domains while, for circular sectors, the radius, the anomalies of the segments defining the sector and the coordinates of the relevant endpoints.

We limit ourselves to computing the 0th-order (mass), 1st-order (static moment), and 2nd-order (inertia tensor) mass moments of polygons and circular sectors although the approach presented in the paper can be applied to generalised mass moments of arbitrary order, i.e. to integrals (1) and (2) for $k > 2$. In addition, the algorithm for computing the 3rd-order mass moment of homogeneous circular sectors is presented.

The main advantage of analytically evaluating the mass moments of functionally graded 2D domains and axisymmetric solids lies in the time saving that can be achieved for linear [34] and nonlinear structural analyses [35,36]; especially in this last case, change in the geometric or material properties obliges to continuously update the computation of the mass moments required to carry out the iterations intrinsic to the nonlinear structural problems. As proved in Subsec. 9.3, even for a much simpler linear analysis, the

use of the analytical formulas derived in the paper reduces the overall computational effort by orders of magnitude with respect to that associated with the use of quadrature formulas.

The paper is organised as follows. A brief overview of the geometric properties of homogeneous domains and their evaluation by means of boundary integrals is presented in Sec. 2.

The mass moments of 2D domains and axisymmetric solids characterised by polynomial, exponential and polynomial quadratic density distributions are expressed as boundary integrals in Secs. 3 and 4, respectively, by exploiting differential identities derived in specific Sections included as Supplementary Material (SM). The analytical evaluation of the relevant boundary integrals by means of algebraic expressions is explicitly carried out in Secs. 5 and 6 for polygonal domains.

The same procedure is repeated in Secs. 7 and 8 for 2D domains and axisymmetric solids shaped as circular sectors by considering density varying along a radial direction either linearly or quadratically.

Finally, the proposed approach is validated in Sec. 9 by comparing the results prompting from the application of the formulas derived in the paper with an analytical or numerical evaluation of the domain integrals.

2. Mass moments of homogeneous 2D domains

To illustrate the rationale of the approach developed in the body of the paper, it is convenient to preliminarily address the computation of the basic geometric properties $\mathbf{J}^{(0)}_{2\Omega}$, $\mathbf{J}^{(1)}_{2\Omega}$ and $\mathbf{J}^{(2)}_{2\Omega}$ of homogeneous 2D domains, i.e. the quantities (1) when $\varrho(\boldsymbol{\rho}) = 1$ and setting in turn $k = 0$, $k = 1$ and $k = 2$. To this end, we recall the following result [14]:

Proposition 2.1. *For a homogeneous 2D domain Ω it turns out to be*

$$\mathbf{J}^{(k)}_{2\Omega} = \frac{1}{2+k}\int_{\partial\Omega} [\otimes\boldsymbol{\rho},\ k]\ (\boldsymbol{\rho}\cdot\mathbf{n})\ \mathrm{d}s = \frac{1}{2+k}\mathbf{J}^{(k)}_{2\,\partial\Omega}, \tag{3}$$

where $\partial\Omega$ is the boundary of Ω and $\mathbf{n}$ is the unit normal pointing outwards. The proof follows from Eq. (A.8) in the SM 1 included as Supplementary Material for this paper.

According to the previous result, we can evaluate the geometric properties of 2D domains by simply computing line integrals. In fact, applying Eq. (3) one has

$$A = \int_{\Omega} \mathrm{d}A = \frac{1}{2}\int_{\partial\Omega} \boldsymbol{\rho}\cdot\mathbf{n}\,\mathrm{d}s = \frac{1}{2}\mathbf{J}^{(0)}_{2\,\partial\Omega}, \tag{4a}$$

$$\mathbf{s}_O = \int_{\Omega} \boldsymbol{\rho}\,\mathrm{d}A = \frac{1}{3}\int_{\partial\Omega} (\boldsymbol{\rho}\cdot\mathbf{n})\,\boldsymbol{\rho}\,\mathrm{d}s = \frac{1}{3}\mathbf{J}^{(1)}_{2\,\partial\Omega}, \tag{4b}$$

$$\mathbf{J}_O = \int_{\Omega} \boldsymbol{\rho}\otimes\boldsymbol{\rho}\,\mathrm{d}A = \frac{1}{4}\int_{\partial\Omega} (\boldsymbol{\rho}\cdot\mathbf{n})\,(\boldsymbol{\rho}\otimes\boldsymbol{\rho})\,\mathrm{d}s = \frac{1}{4}\mathbf{J}^{(2)}_{2\,\partial\Omega}, \tag{4c}$$

that provide very useful expressions for the area A ($k = 0$), static moment $\mathbf{s}_O$ ($k = 1$) and inertia tensor $\mathbf{J}_O$ ($k = 2$) of homogeneous 2D domains.

Actually, in the frequent case of polygonal domains, the aforementioned mass moments can be computed analytically by means of expressions depending upon the vectors $\boldsymbol{\rho}_i$, $\boldsymbol{\rho}_{i+1}$ that collect the coordinates of the vertices i and $i+1$, endpoints of the i-th side, and the relevant unit normal $\mathbf{n}_i$, see, e.g., Fig. 1. In particular, denoting by s_i the curvilinear abscissa along the i-th side having origin at i-th vertex, we set $\lambda_i = s_i/l_i$, where l_i is the length of the i-th side, and

$$\boldsymbol{\rho}(s_i(\lambda_i)) = \tilde{\boldsymbol{\rho}}(\lambda_i) = \boldsymbol{\rho}_i\,\left(1-\lambda_i\right) + \boldsymbol{\rho}_{i+1}\,\lambda_i;$$

furthermore,

$$\mathbf{n}_i = \frac{\left(\boldsymbol{\rho}_{i+1}-\boldsymbol{\rho}_i\right)^{\perp}}{\|\boldsymbol{\rho}_{i+1}-\boldsymbol{\rho}_i\|} = \frac{\Delta\boldsymbol{\rho}_i^{\perp}}{l_i},$$

where the symbol $\perp$ represents the clockwise rotated of the vector $\Delta\boldsymbol{\rho}_i$ so that $\mathbf{n}_i$ points outwards Ω. This convention is a consequence of numbering the vertices of $\partial\Omega$ in a counter-clockwise sense.

A simple example of the previous path of reasoning is represented by the algebraic counterpart of the formulas (4). Although the relevant expressions are available in the literature [14] it is instructive to report them explicitly since the formulas derived later for arbitrary density distributions represent their generalisation.

In particular, observing that

$$\tilde{\boldsymbol{\rho}}(\lambda_i)\cdot\mathbf{n}_i = \boldsymbol{\rho}_i\cdot\frac{\Delta\boldsymbol{\rho}_i^{\perp}}{l_i} = \frac{\boldsymbol{\rho}_i\cdot\boldsymbol{\rho}_{i+1}^{\perp}}{l_i}, \tag{5}$$

it turns out to be

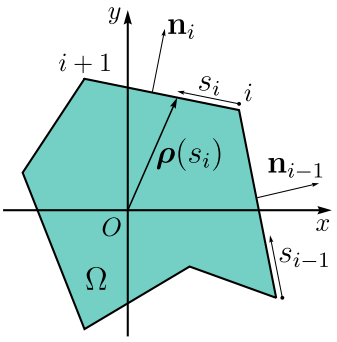

Fig. 1. A polygonal domain.

$$
\begin{aligned}
A &= \frac{1}{2}\,\mathbf{J}^{(0)}_{2\,\partial\Omega} = \frac{1}{2}\sum_{i=1}^{n} c_i,\\
\mathbf{s}_O &= \frac{1}{3}\,\mathbf{J}^{(1)}_{2\,\partial\Omega} = \frac{1}{6}\sum_{i=1}^{n} c_i\,(\boldsymbol{\rho}_i + \boldsymbol{\rho}_{i+1}),\\
\mathbf{J}_O &= \frac{1}{4}\,\mathbf{J}^{(2)}_{2\,\partial\Omega} = \frac{1}{12}\sum_{i=1}^{n} c_i\,\left[\mathbf{P}_i + \frac{1}{2}\,\mathbf{P}_{i,i+1} + \mathbf{P}_{i+1}\right],
\end{aligned}
\tag{6}
$$

where it has been set

$$
c_i = \boldsymbol{\rho}_i \cdot \boldsymbol{\rho}^{\perp}_{i+1}, \quad \mathbf{P}_{i,i+1} = \boldsymbol{\rho}_i \otimes \boldsymbol{\rho}_{i+1} + \boldsymbol{\rho}_{i+1} \otimes \boldsymbol{\rho}_i, \quad \mathbf{P}_i = \boldsymbol{\rho}_i \otimes \boldsymbol{\rho}_i,
\tag{7}
$$

while the expression of $\mathbf{P}_{i+1}$ directly stems from that of $\mathbf{P}_i$.

The notation just introduced will be particularly useful in the sequel to provide compact expressions of the generalised mass moments associated with complex density distributions.

3. Functionally graded 2D domains: expressions for boundary integrals

Aim of this Section is to express the mass moments (1) by means of boundary integrals for

• a polynomial density distribution

$$
\varrho^{\mathrm{pln}}(\boldsymbol{\rho}) = \sum_{q=0}^{m} C_q\,(\boldsymbol{\rho}\cdot\mathbf{a})^q\,,
\tag{8}
$$

where $C_0, C_1, \ldots, C_m$ are real coefficients, m is a non-negative integer and $\mathbf{a}$ is a unit vector defining the direction along which the density is varying.

• an exponential density distribution

$$
\varrho^{\mathrm{exp}}(\boldsymbol{\rho}) = e^{\alpha\,\boldsymbol{\rho}\cdot\mathbf{a}},
\tag{9}
$$

where α is a real coefficient.

• a polynomial quadratic density distribution

$$
\varrho^{\mathrm{plq}}(\boldsymbol{\rho}) = \sum_{q=0}^{m} C_q\,(\boldsymbol{\rho}\cdot\boldsymbol{\rho})^q = \sum_{q=0}^{m} C_q\,\|\boldsymbol{\rho}\|^{2q}.
\tag{10}
$$

In particular, we are going to derive formulas analogous to (6) in which both the constant c_i and the quantities $\boldsymbol{\rho}_i$, $\boldsymbol{\rho}_{i+1}$, $\mathbf{P}_i$, $\mathbf{P}_{i,i+1}$ and $\mathbf{P}_{i+1}$ will be scaled by further constants depending upon the order of the moment to be computed and the coefficients defining the density distribution.

All formulas derived in the sequel are based upon suitable applications of Gauss theorem and the relevant proofs are included in the Supplementary Material section which the interested reader is referred to.

3.1. Polynomial density distribution

The integrals (1) specialise as follows

$$
\mathbf{J}^{(k),\mathrm{pln}}_{2\,\Omega} = \sum_{q=0}^{m} C_q \int_{\Omega} (\boldsymbol{\rho}\cdot\mathbf{a})^q\,[\otimes\boldsymbol{\rho},\ k]\,\mathrm{d}A,
$$

so that, introducing the notation

$$D_p^{(kj)} = \frac{C_q}{p+k+j}, \tag{11}$$

where p (j) is a non-negative (positive) integer, the following result can be profitably invoked:

Proposition 3.1. *Let Ω be a 2D domain characterised by a polynomial density expressed by the formula (8). The k-order moment can be expressed as an integral extended to the boundary $\partial\Omega$ by means of the formula*

$$\mathbf{J}_{2\Omega}^{(k),\mathrm{pln}} = \sum_{q=0}^{m} D_q^{(k2)} \int_{\partial\Omega} (\boldsymbol{\rho}\cdot\mathbf{a})^q \, (\boldsymbol{\rho}\cdot\mathbf{n}) \, [\otimes\boldsymbol{\rho},\ k] \, \mathrm{d}s = \sum_{q=0}^{m} D_q^{(k2)} \, \mathbf{J}_{2\partial\Omega}^{(k),\mathrm{pln}}. \tag{12}$$

The previous identity, whose proof can be inferred from Eq. (B.1) in the SM 2, can be specialised in a straightforward manner to the cases of greater interest, that is $k=0$, $k=1$ and $k=2$, although the relevant expressions can also be obtained directly from Eqs. (B.2), (B.3) and (B.4), respectively.

The boundary integrals associated with the specialisation of formula (12), namely

$$\mathbf{J}_{2\partial\Omega}^{(0),\mathrm{pln}} = \int_{\partial\Omega} (\boldsymbol{\rho}\cdot\mathbf{a})^q \, (\boldsymbol{\rho}\cdot\mathbf{n}) \, \mathrm{d}s, \tag{13a}$$

$$\mathbf{J}_{2\partial\Omega}^{(1),\mathrm{pln}} = \int_{\partial\Omega} (\boldsymbol{\rho}\cdot\mathbf{a})^q \, (\boldsymbol{\rho}\cdot\mathbf{n}) \, \boldsymbol{\rho} \, \mathrm{d}s, \tag{13b}$$

$$\mathbf{J}_{2\partial\Omega}^{(2),\mathrm{pln}} = \int_{\partial\Omega} (\boldsymbol{\rho}\cdot\mathbf{a})^q \, (\boldsymbol{\rho}\cdot\mathbf{n}) \, (\boldsymbol{\rho}\otimes\boldsymbol{\rho}) \, \mathrm{d}s, \tag{13c}$$

are explicitly computed in Sec. 5 and reported in Eqs. (23), (25) and (27) for polygonal domains.

3.2. Exponential density distribution

According to (9), formula (1) specialises to

$$\mathbf{J}_{2\Omega}^{(k),\mathrm{exp}} = \int_{\Omega} e^{\alpha\,\boldsymbol{\rho}\cdot\mathbf{a}} \, [\otimes\boldsymbol{\rho},\ k] \, \mathrm{d}A,$$

for which it is advantageous to exploit the following result

Proposition 3.2. *Assuming that Ω is a functionally graded 2D domain characterised by an exponential density distribution (9), the k-order moment can be expressed as a function of integrals extended to the boundary $\partial\Omega$ by means of the formula*

$$\mathbf{J}_{2\Omega}^{(k),\mathrm{exp}} = \left[\int_{\partial\Omega} e^{\alpha\,\boldsymbol{\rho}\cdot\mathbf{a}} \, [\otimes\boldsymbol{\rho},\ k] \otimes \mathbf{n} \, \mathrm{d}s\right] \frac{\mathbf{a}}{\alpha} - \mathbf{A}\left(\mathbf{J}_{2\Omega}^{(k-1),\mathrm{exp}}, \ldots, \mathbf{J}_{2\Omega}^{(0),\mathrm{exp}}\right) = \mathbf{J}_{2\partial\Omega}^{(k),\mathrm{exp}} \frac{\mathbf{a}}{\alpha} - \mathbf{A}\left(\mathbf{J}_{2\Omega}^{(k-1),\mathrm{exp}}, \ldots, \mathbf{J}_{2\Omega}^{(0),\mathrm{exp}}\right), \tag{14}$$

where $\mathbf{A}$ is a tensor function, depending on lower-order mass moments, that is null for $k=0$.

The previous result, that follows from identity (B.6), basically states that the mass moment of order $k \geq 1$ can be obtained by computing only boundary integrals since each one of the lower order moments $\mathbf{J}_{2\Omega}^{(k-1),\mathrm{exp}}$ can in turn be computed by means of boundary integrals.

Specifically, invoking formula (B.14), (B.15) and (B.16) in the SM 2 as well as formulas (A.1l) and (A.1m) in the SM 1, one has

$$\mathbf{J}_{2\Omega}^{(0),\mathrm{exp}} = \left[\int_{\partial\Omega} e^{\alpha\,\boldsymbol{\rho}\cdot\mathbf{a}} \, \mathbf{n} \, \mathrm{d}s\right] \cdot \frac{\mathbf{a}}{\alpha}, \tag{15a}$$

$$\mathbf{J}_{2\Omega}^{(1),\mathrm{exp}} = \left[\int_{\partial\Omega} e^{\alpha\,\boldsymbol{\rho}\cdot\mathbf{a}} \, (\boldsymbol{\rho}\otimes\mathbf{n}) \, \mathrm{d}s\right] \frac{\mathbf{a}}{\alpha} - \mathbf{J}_{2\Omega}^{(0),\mathrm{exp}} \frac{\mathbf{a}}{\alpha}, \tag{15b}$$

$$\mathbf{J}_{2\Omega}^{(2),\mathrm{exp}} = \left[\int_{\partial\Omega} e^{\alpha\,\boldsymbol{\rho}\cdot\mathbf{a}} \, (\boldsymbol{\rho}\otimes\boldsymbol{\rho}\otimes\mathbf{n}) \, \mathrm{d}s\right] \frac{\mathbf{a}}{\alpha} - \mathbf{J}_{2\Omega}^{(1),\mathrm{exp}} \otimes \frac{\mathbf{a}}{\alpha} - \frac{\mathbf{a}}{\alpha} \otimes \mathbf{J}_{2\Omega}^{(1),\mathrm{exp}}. \tag{15c}$$

The specialisation of the previous formulas to the case of polygonal domains is detailed in Sec. 5, while the analytical formulas for their evaluation are reported in Eqs. (30), (32) and (34).

3.3. Polynomial quadratic density distribution

Invoking (10), formula (1) provides

$$\mathbf{J}_{2\,\Omega}^{(k),\mathrm{plq}} = \sum_{q=0}^{m} C_q \int_{\Omega} (\boldsymbol{\rho}\cdot\boldsymbol{\rho})^q \, [\otimes\boldsymbol{\rho},\ k]\,\mathrm{d}A,$$

so that the identity (B.18) yields

Proposition 3.3. *Given a 2D domain Ω having a polynomial density specified by Eq. (10), the k-order moment can be computed by means of boundary integrals defined by*

$$\mathbf{J}_{2\,\Omega}^{(k),\mathrm{plq}} = \sum_{q=0}^{m} D_{2\,q}^{(k2)} \int_{\partial\Omega} (\boldsymbol{\rho}\cdot\boldsymbol{\rho})^q \, (\boldsymbol{\rho}\cdot\mathbf{n}) \, [\otimes\boldsymbol{\rho},\ k]\,\mathrm{d}s = \sum_{q=0}^{m} D_{2\,q}^{(k2)} \, \mathbf{J}_{2\,\partial\Omega}^{(k),\mathrm{plq}}.$$

Hence, for the cases of greater interest, e.g. $k = 0, 1, 2$, one has

$$\mathbf{J}_{2\,\Omega}^{(0),\mathrm{plq}} = \sum_{q=0}^{m} D_{2\,q}^{(02)} \int_{\partial\Omega} (\boldsymbol{\rho}\cdot\boldsymbol{\rho})^q \, (\boldsymbol{\rho}\cdot\mathbf{n}) \,\mathrm{d}s, \tag{16a}$$

$$\mathbf{J}_{2\,\Omega}^{(1),\mathrm{plq}} = \sum_{q=0}^{m} D_{2\,q}^{(12)} \int_{\partial\Omega} (\boldsymbol{\rho}\cdot\boldsymbol{\rho})^q \, (\boldsymbol{\rho}\cdot\mathbf{n}) \, \boldsymbol{\rho}\,\mathrm{d}s, \tag{16b}$$

$$\mathbf{J}_{2\,\Omega}^{(2),\mathrm{plq}} = \sum_{q=0}^{m} D_{2\,q}^{(22)} \int_{\partial\Omega} (\boldsymbol{\rho}\cdot\boldsymbol{\rho})^q \, (\boldsymbol{\rho}\cdot\mathbf{n}) \, (\boldsymbol{\rho}\otimes\boldsymbol{\rho}) \,\mathrm{d}s, \tag{16c}$$

and the analytical evaluation of the boundary integrals for polygonal domains will be addressed in Sec. 5. For the reader's convenience, the relevant formulas can be found in Eqs. (36).

4. Functionally graded axisymmetric solids: expressions for boundary integrals

In the following Subsections, we derive the expressions for boundary integrals of the generalised mass moments (2) for axisymmetric solids endowed with the density functions reported in Sec. 3.

Indeed, the formulas derived in the previous Section are valid for axisymmetric solids as well, apart from the constant $2\,\pi$, as long as $\mathbf{a}$ coincides with the unit vector $\mathbf{b}$ orthogonal to the axis of revolution. However, for greater generality, we shall assume $\mathbf{a} \neq \mathbf{b}$.

4.1. Polynomial density distribution

The k-order mass moment of an axisymmetric domain characterised by a polynomial density distribution expressed by Eq. (8) is defined as

$$\mathbf{J}_{\mathrm{ax}\,\Omega}^{(k),\mathrm{pln}} = 2\,\pi \sum_{q=0}^{m} C_q \int_{\Omega} (\boldsymbol{\rho}\cdot\mathbf{a})^q \, (\boldsymbol{\rho}\cdot\mathbf{b}) \, [\otimes\boldsymbol{\rho},\ k]\,\mathrm{d}A.$$

For its computation, the following result is beneficial:

Proposition 4.1. *Assuming Ω to be a functionally graded axisymmetric domain, characterised by a polynomial density defined by Eq. (8), the k-order moment can be represented as a function of integrals that are extended to the boundary $\partial\Omega$*

$$\mathbf{J}_{\mathrm{ax}\,\Omega}^{(k),\mathrm{pln}} = 2\,\pi \sum_{q=0}^{m} D_{q}^{(k3)} \int_{\partial\Omega} (\boldsymbol{\rho}\cdot\mathbf{a})^q \, (\boldsymbol{\rho}\cdot\mathbf{b}) \, (\boldsymbol{\rho}\cdot\mathbf{n}) \, [\otimes\boldsymbol{\rho},\ k]\,\mathrm{d}s = 2\,\pi \sum_{q=0}^{m} D_{q}^{(k3)} \, \mathbf{J}_{\mathrm{ax}\,\partial\Omega}^{(k),\mathrm{pln}}. \tag{17}$$

The proof follows from Eq. (C.1) in the SM 3, the constant $D_q^{(k3)}$ being defined in (11). The previous identity can be specialised to the most important cases, namely $k = 0$, $k = 1$ and $k = 2$, in the following way

$$\mathbf{J}_{\mathrm{ax}\,\partial\Omega}^{(0),\mathrm{pln}} = \int_{\partial\Omega} (\boldsymbol{\rho}\cdot\mathbf{a})^q \, (\boldsymbol{\rho}\cdot\mathbf{b}) \, (\boldsymbol{\rho}\cdot\mathbf{n}) \,\mathrm{d}s, \tag{18a}$$

$$\mathbf{J}_{\mathrm{ax}\,\partial\Omega}^{(1),\mathrm{pln}} = \int_{\partial\Omega} (\boldsymbol{\rho}\cdot\mathbf{a})^q \, (\boldsymbol{\rho}\cdot\mathbf{b}) \, (\boldsymbol{\rho}\cdot\mathbf{n}) \, \boldsymbol{\rho}\,\mathrm{d}s, \tag{18b}$$

$$\mathbf{J}^{(2),\mathrm{pln}}_{\mathrm{ax}\,\partial\Omega} = \int_{\partial\Omega} (\boldsymbol{\rho}\cdot\mathbf{a})^q\ (\boldsymbol{\rho}\cdot\mathbf{b})\ (\boldsymbol{\rho}\cdot\mathbf{n})\ (\boldsymbol{\rho}\otimes\boldsymbol{\rho})\ \mathrm{d}s. \tag{18c}$$

In addition, the previous integrals are computed explicitly in Sec. 6 and reported in Eqs. (37), (40) and (42) for axisymmetric polygonal solids.

4.2. Exponential density distribution

The mass moment of order-k, defined by

$$\mathbf{J}^{(k),\mathrm{exp}}_{\mathrm{ax}\,\Omega} = 2\,\pi \int_{\Omega} e^{\alpha\,\boldsymbol{\rho}\cdot\mathbf{a}}\ (\boldsymbol{\rho}\cdot\mathbf{b})\ [\otimes\boldsymbol{\rho},\ k]\,\mathrm{d}A,$$

can be expressed in terms of boundary integrals on account of the following

Proposition 4.2. *Under the assumption that Ω is a functionally graded axisymmetric domain, characterised by an exponential density distribution (9), the k-order moment can be expressed as a function of integrals that are extended to the boundary $\partial\Omega$ by means of*

$$\begin{aligned}\mathbf{J}^{(k),\mathrm{exp}}_{\mathrm{ax}\,\Omega} &= 2\,\pi \left[\int_{\partial\Omega} e^{\alpha\,\boldsymbol{\rho}\cdot\mathbf{a}}\ (\boldsymbol{\rho}\cdot\mathbf{b})\ [\otimes\boldsymbol{\rho},\ k]\otimes\mathbf{n}\,\mathrm{d}s\right]\frac{\mathbf{a}}{\alpha} - \mathbf{A}\left(2\,\pi\,\mathbf{J}^{(k),\mathrm{exp}}_{2\,\Omega}, \mathbf{J}^{(k-1),\mathrm{exp}}_{\mathrm{ax}\,\Omega}, \dots, \mathbf{J}^{(0),\mathrm{exp}}_{\mathrm{ax}\,\Omega}\right) = \\ &= 2\,\pi\,\mathbf{J}^{(k),\mathrm{exp}}_{\mathrm{ax}\,\partial\Omega}\frac{\mathbf{a}}{\alpha} - \mathbf{A}\left(2\,\pi\,\mathbf{J}^{(k),\mathrm{exp}}_{2\,\Omega}, \mathbf{J}^{(k-1),\mathrm{exp}}_{\mathrm{ax}\,\Omega}, \dots, \mathbf{J}^{(0),\mathrm{exp}}_{\mathrm{ax}\,\Omega}\right),\end{aligned}$$

where the tensor function $\mathbf{A}$ is dependent both on the lower-order mass moments and on the moment $\mathbf{J}^{(k),\mathrm{exp}}_{2\Omega}$ defined in Eq. (14).

The proof of the previous proposition can be derived from Eq. (C.6) in the SM 3. Accordingly, the expressions for the mass moments of order $k = 0, 1, 2$ of axisymmetric solids are given by

$$\mathbf{J}^{(0),\mathrm{exp}}_{\mathrm{ax}\,\Omega} = 2\,\pi \left\{\left[\int_{\partial\Omega} e_{\mathbf{ab}}\,\mathbf{n}\,\mathrm{d}s\right]\cdot\frac{\mathbf{a}}{\alpha} - \mathbf{J}^{(0),\mathrm{exp}}_{2\,\Omega}\left(\frac{\mathbf{a}}{\alpha}\cdot\mathbf{b}\right)\right\}, \tag{19a}$$

$$\mathbf{J}^{(1),\mathrm{exp}}_{\mathrm{ax}\,\Omega} = 2\,\pi \left\{\left[\int_{\partial\Omega} e_{\mathbf{ab}}\ (\boldsymbol{\rho}\otimes\mathbf{n})\,\mathrm{d}s\right]\frac{\mathbf{a}}{\alpha} - \mathbf{J}^{(1),\mathrm{exp}}_{2\,\Omega}\left(\frac{\mathbf{a}}{\alpha}\cdot\mathbf{b}\right)\right\} - \mathbf{J}^{(0),\mathrm{exp}}_{\mathrm{ax}\,\Omega}\frac{\mathbf{a}}{\alpha}, \tag{19b}$$

$$\mathbf{J}^{(2),\mathrm{exp}}_{\mathrm{ax}\,\Omega} = 2\,\pi \left\{\left[\int_{\partial\Omega} e_{\mathbf{ab}}\ (\boldsymbol{\rho}\otimes\boldsymbol{\rho}\otimes\mathbf{n})\,\mathrm{d}s\right]\frac{\mathbf{a}}{\alpha} - \mathbf{J}^{(2),\mathrm{exp}}_{2\,\Omega}\left(\frac{\mathbf{a}}{\alpha}\cdot\mathbf{b}\right)\right\} - \mathbf{J}^{(1),\mathrm{exp}}_{\mathrm{ax}\,\Omega}\otimes\frac{\mathbf{a}}{\alpha} - \frac{\mathbf{a}}{\alpha}\otimes\mathbf{J}^{(1),\mathrm{exp}}_{\mathrm{ax}\,\Omega}, \tag{19c}$$

in which $e_{\mathbf{ab}} = e^{\alpha\,\boldsymbol{\rho}\cdot\mathbf{a}}\ (\boldsymbol{\rho}\cdot\mathbf{b})$ while $\mathbf{J}^{(0),\mathrm{exp}}_{2\,\Omega}$, $\mathbf{J}^{(1),\mathrm{exp}}_{2\,\Omega}$, $\mathbf{J}^{(2),\mathrm{exp}}_{2\,\Omega}$ are defined in Eqs. (15).

Furthermore, the aforementioned integrals are explicitly computed in Sec. 6 and presented in Eqs. (44), (45), and (46) for axisymmetric polygonal solids.

4.3. Polynomial quadratic density distribution

The k-order mass moment of an axisymmetric domain endowed with the density distribution (10) is defined as

$$\mathbf{J}^{(k),\mathrm{plq}}_{\mathrm{ax}\,\Omega} = 2\,\pi \sum_{q=0}^{m} C_q \int_{\Omega} (\boldsymbol{\rho}\cdot\boldsymbol{\rho})^q\ (\boldsymbol{\rho}\cdot\mathbf{b})\ [\otimes\boldsymbol{\rho},\ k]\,\mathrm{d}A.$$

The mass moment can be converted to the sum of integrals extended to the boundary $\partial\Omega$ by invoking the identity (C.13) established in the SM 3. Hence, one can state the following

Proposition 4.3. *Given an axisymmetric domain Ω having the polynomial quadratic density distribution specified by Eq. (10), the k-order moment can be computed as*

$$\mathbf{J}^{(k),\mathrm{plq}}_{\mathrm{ax}\,\Omega} = 2\,\pi \sum_{q=0}^{m} D^{(k3)}_{2\,q} \int_{\partial\Omega} (\boldsymbol{\rho}\cdot\boldsymbol{\rho})^q\ (\boldsymbol{\rho}\cdot\mathbf{b})\ (\boldsymbol{\rho}\cdot\mathbf{n})\ [\otimes\boldsymbol{\rho},\ k]\,\mathrm{d}s.$$

Accordingly, one has

$$\mathbf{J}^{(0),\mathrm{plq}}_{\mathrm{ax}\,\Omega} = 2\,\pi \sum_{q=0}^{m} D^{(03)}_{2\,q} \int_{\partial\Omega} (\boldsymbol{\rho}\cdot\boldsymbol{\rho})^q\,(\boldsymbol{\rho}\cdot\mathbf{b})\,(\boldsymbol{\rho}\cdot\mathbf{n})\,\mathrm{d}s,$$
$$\mathbf{J}^{(1),\mathrm{plq}}_{\mathrm{ax}\,\Omega} = 2\,\pi \sum_{q=0}^{m} D^{(13)}_{2\,q} \int_{\partial\Omega} (\boldsymbol{\rho}\cdot\boldsymbol{\rho})^q\,(\boldsymbol{\rho}\cdot\mathbf{b})\,(\boldsymbol{\rho}\cdot\mathbf{n})\,\boldsymbol{\rho}\,\mathrm{d}s, \tag{20}$$
$$\mathbf{J}^{(2),\mathrm{plq}}_{\mathrm{ax}\,\Omega} = 2\,\pi \sum_{q=0}^{m} D^{(23)}_{2\,q} \int_{\partial\Omega} (\boldsymbol{\rho}\cdot\boldsymbol{\rho})^q\,(\boldsymbol{\rho}\cdot\mathbf{b})\,(\boldsymbol{\rho}\cdot\mathbf{n})\,(\boldsymbol{\rho}\otimes\boldsymbol{\rho})\,\mathrm{d}s.$$

The above-mentioned integrals are explicitly evaluated in Sec. 6 and presented in Eqs. (47) for the significant case of axisymmetric polygonal solids.

5. Evaluation of boundary integrals for functionally graded polygonal domains

The formulas developed in the previous Sections have allowed us to prove that the domain integrals involved in the definition of the generalised mass moments can be expressed as a function of boundary integrals, i.e. integrals extended to the boundary of the original domain.

Aim of this Section is to show how the boundary integrals can be evaluated analytically by means of algebraic formulas depending solely upon the coefficients appearing in the density function and the coordinates of the vertices defining the boundary $\partial\Omega$ of a polygonal domain Ω, see, e.g., Fig. 1.

Denoting by n the number of vertices of $\partial\Omega$, by $\partial\Omega_i$ the generic side of $\partial\Omega$ and assuming that the vertices are numbered consecutively by traversing the boundary of Ω in counter-clockwise sense, the integral of a generic function f defined on $\partial\Omega$ can be computed as follows

$$\int_{\partial\Omega} f(s)\,\mathrm{d}s = \sum_{i=1}^{n} \int_{\partial\Omega_i} f(s_i)\,\mathrm{d}s_i = \sum_{i=1}^{n} \int_{0}^{l_i} f(s_i)\,\mathrm{d}s_i = \sum_{i=1}^{n} \int_{0}^{1} \tilde{f}(\lambda_i)\,\mathrm{d}\lambda_i\,l_i, \tag{21}$$

where $\tilde{f} = f\circ s$.

For the cases of interest, the function f is given by tensor expressions depending upon the vector $\boldsymbol{\rho}$ spanning the i-th side and the relevant unit normal $\mathbf{n}_i$.

5.1. Polynomial density

Let us assume that the polygonal domain Ω is endowed with a polynomial density distribution given by (8) and that the boundary integrals $\mathbf{J}^{(0),\mathrm{pln}}_{2\,\partial\Omega}$, $\mathbf{J}^{(1),\mathrm{pln}}_{2\,\partial\Omega}$ and $\mathbf{J}^{(2),\mathrm{pln}}_{2\,\partial\Omega}$ defined in Eqs. (13) need to be evaluated.

Accordingly, we make use of the following result

$$\left(\tilde{\boldsymbol{\rho}}(\lambda_i)\cdot\mathbf{a}\right)^q = \sum_{r=0}^{q} \binom{q}{r} \left(\boldsymbol{\rho}_i\cdot\mathbf{a}\right)^{q-r} \left(1-\lambda_i\right)^{q-r} \left(\boldsymbol{\rho}_{i+1}\cdot\mathbf{a}\right)^{r} \lambda_i^r = \sum_{r=0}^{q} \binom{q}{r} a_i^{q-r} \left(1-\lambda_i\right)^{q-r} a_{i+1}^{r}\,\lambda_i^r, \tag{22}$$

stemming from the Binomial Theorem, so that (13a) yields

$$\mathbf{J}^{(0),\mathrm{pln}}_{2\,\partial\Omega} = \frac{1}{q+1} \sum_{i=1}^{n} c_i \sum_{r=0}^{q} a_i^{q-r}\,a_{i+1}^{r}, \tag{23}$$

the coefficient c_i being defined in Eq. (7). Hence, on account of (12), it turns out to be

$$\mathbf{J}^{(0),\mathrm{pln}}_{2\,\Omega} = \sum_{q=0}^{m} D^{P\,(2)}_{q} \sum_{i=1}^{n} c_i \sum_{r=0}^{q} a_i^{q-r}\,a_{i+1}^{r}, \tag{24}$$

where

$$D^{P\,(j)}_{q} = \frac{C_q}{(q+1)\,(q+2)\ldots(q+j)} = C_q\,P^{(j)}_{1/q},$$

and j is a positive integer.

Furthermore, the boundary integral $\mathbf{J}^{(1),\mathrm{pln}}_{2\,\partial\Omega}$ in (13b) becomes

$$\mathbf{J}^{(1),\mathrm{pln}}_{2\,\partial\Omega} = P^{(2)}_{1/q} \sum_{i=1}^{n} c_i \sum_{r=0}^{q} a_i^{q-r}\,a_{i+1}^{r}\,[(q-r+1)\,\boldsymbol{\rho}_i + (r+1)\,\boldsymbol{\rho}_{i+1}], \tag{25}$$

so that, recalling (12), the associated domain integral $\mathbf{J}^{(1),\mathrm{pln}}_{2\,\Omega}$ is given by

$$\mathbf{J}_{2\Omega}^{(1),\mathrm{pln}} = \sum_{q=0}^{m} D_q^{P\,(3)} \sum_{i=1}^{n} c_i \sum_{r=0}^{q} a_i^{q-r}\, a_{i+1}^{r} \left[\prod_{q-r}^{1} \boldsymbol{\rho}_i + \prod_{r}^{1} \boldsymbol{\rho}_{i+1} \right]. \tag{26}$$

Finally, we infer from (13c) that

$$\mathbf{J}_{2\partial\Omega}^{(2),\mathrm{pln}} = P_{1/q}^{(3)} \sum_{i=1}^{n} c_i \sum_{r=0}^{q} a_i^{q-r}\, a_{i+1}^{r} \left[\prod_{q-r}^{2} \mathbf{P}_i + \prod_{q-r}^{1} \prod_{r}^{1} \mathbf{P}_{i,i+1} + \prod_{r}^{2} \mathbf{P}_{i+1} \right]. \tag{27}$$

In conclusion, invoking Eq. (12), the domain integral $\mathbf{J}_{2\Omega}^{(2),\mathrm{pln}}$ can be expressed as follows

$$\mathbf{J}_{2\Omega}^{(2),\mathrm{pln}} = \sum_{q=0}^{m} D_q^{P\,(4)} \sum_{i=1}^{n} c_i \sum_{r=0}^{q} a_i^{q-r}\, a_{i+1}^{r} \left[\prod_{q-r}^{2} \mathbf{P}_i + \prod_{q-r}^{1} \prod_{r}^{1} \mathbf{P}_{i,i+1} + \prod_{r}^{2} \mathbf{P}_{i+1} \right]. \tag{28}$$

5.2. Exponential density

In the sequel the line integrals in (15) are evaluated as a function of the coordinates of the vertices of a domain Ω having an arbitrary polygonal shape. The mass moments can be evaluated by using the transformation (21), formula (5) and integrating by parts. Specifically, it turns out to be

$$\mathbf{J}_{2\Omega}^{(0),\mathrm{exp}} = \sum_{i=1}^{n} \frac{e^{\alpha\, a_i} - e^{\alpha\, a_{i+1}}}{\alpha\,(a_i - a_{i+1})}\, \Delta\boldsymbol{\rho}_i^{\perp} \cdot \frac{\mathbf{a}}{\alpha} \qquad \text{iff} \quad a_i \neq a_{i+1}, \tag{29}$$

where a_i and a_{i+1} have been defined in (22).

The generic addend of the sum in formula (29) is not defined when $a_i = a_{i+1}$, i.e. when the i-th side of the polygon is orthogonal to the vector $\mathbf{a}$ along which the density varies. Along this special side (SS) the quantity $e^{\alpha\,\boldsymbol{\rho}\cdot\mathbf{a}}$ is constant so that the contribution to the integral (15a) provided by SS becomes

$$\int_{SS} e^{\alpha\,\boldsymbol{\rho}\cdot\mathbf{a}}\, \mathbf{n}\, \mathrm{d}s = e^{\alpha\, a_i} \int_{SS} \mathbf{n}\, \mathrm{d}s = e^{\alpha\, a_i}\, \Delta\boldsymbol{\rho}_{SS}^{\perp},$$

since the constant $e^{\alpha\,\boldsymbol{\rho}\cdot\mathbf{a}}$ attains the same value whatever is the vector considered along SS. Accordingly, formula (29) is conveniently reformulated as follows

$$\mathbf{J}_{2\Omega}^{(0),\mathrm{exp}} = \sum_{i=1}^{n} \begin{cases} \dfrac{e^{\alpha\, a_i} - e^{\alpha\, a_{i+1}}}{\alpha\,(a_i - a_{i+1})}\, \Delta\boldsymbol{\rho}_i^{\perp} \cdot \dfrac{\mathbf{a}}{\alpha} & \text{iff} \quad a_i \neq a_{i+1}, \\ e^{\alpha\, a_i}\, \Delta\boldsymbol{\rho}_i^{\perp} \cdot \dfrac{\mathbf{a}}{\alpha} & \text{iff} \quad a_i = a_{i+1}. \end{cases} \tag{30}$$

In order to evaluate the integral $\mathbf{J}_{2\Omega}^{(1),\mathrm{exp}}$ in Eq. (15b), it is convenient to introduce the following notation

$$e_{(i)d,f}^{(c)} = e^{\alpha\, a_i}\, [\alpha\, d\, (a_i - a_{i+1}) - f]^c, \qquad e_{-(i)d,f}^{(c)} = e^{\alpha\, a_i}\, [\alpha\, d\, (a_{i+1} - a_i) - f]^c,$$
$$e_{(i+1)d,f}^{(c)} = e^{\alpha\, a_{i+1}}\, [\alpha\, d\, (a_i - a_{i+1}) - f]^c, \qquad e_{-(i+1)d,f}^{(c)} = e^{\alpha\, a_{i+1}}\, [\alpha\, d\, (a_{i+1} - a_i) - f]^c,$$

where c, d and f are integers.

Assuming $a_i \neq a_{i+1}$ the contribution provided by the i-th side to the boundary integral in Eq. (15b) becomes

$$\mathbf{J}_{2\partial\Omega_i}^{(1),\mathrm{exp}} = [(\Psi_1\, \boldsymbol{\rho}_i + \Psi_2\, \boldsymbol{\rho}_{i+1}) \otimes \Delta\boldsymbol{\rho}_i^{\perp}]\, \frac{\mathbf{a}}{\alpha}, \quad a_i \neq a_{i+1},$$

where

$$\Psi_1 = \frac{e^{\alpha\, a_{i+1}} + e_{(i)1,1}^{(1)}}{\alpha^2 (a_i - a_{i+1})^2}, \qquad \Psi_2 = \frac{e^{\alpha\, a_i} + e_{-(i+1)1,1}^{(1)}}{\alpha^2 (a_i - a_{i+1})^2}, \qquad a_i \neq a_{i+1}. \tag{31}$$

Whereas, should it be $a_i = a_{i+1}$, one can infer

$$\mathbf{J}_{2\partial\Omega_{SS}}^{(1),\mathrm{exp}} = \frac{e^{\alpha\, a_i}}{2}\, \left[(\boldsymbol{\rho}_i + \boldsymbol{\rho}_{i+1}) \otimes \Delta\boldsymbol{\rho}_i^{\perp}\right]\, \frac{\mathbf{a}}{\alpha}, \qquad a_i = a_{i+1}.$$

Hence, introducing the quantity

$$\mathbf{J}_{2\partial\Omega_{\mathrm{tbs}}}^{(1),\mathrm{exp}} = \begin{cases} \mathbf{J}_{2\partial\Omega_i}^{(1),\mathrm{exp}} & \text{iff} \quad a_i \neq a_{i+1}, \\ \mathbf{J}_{2\partial\Omega_{SS}}^{(1),\mathrm{exp}} & \text{iff} \quad a_i = a_{i+1}, \end{cases}$$

it turns out to be

$$\mathbf{J}^{(1),\exp}_{2\,\Omega} = \sum_{i=1}^{n} \mathbf{J}^{(1),\exp}_{2\,\partial\Omega_{\text{tbs}}} - \mathbf{J}^{(0),\exp}_{2\,\Omega}\,\frac{\mathbf{a}}{\alpha}, \tag{32}$$

where $\mathbf{J}^{(0),\exp}_{2\Omega}$ is given by (30).

If $a_i \neq a_{i+1}$, the evaluation of the boundary integral in (15c) along the i-th side of $\partial\Omega$ is provided by

$$\mathbf{J}^{(2),\exp}_{2\,\partial\Omega_i} = \left\{ \left[\mathbf{P}_i\,\Psi_3 + \mathbf{P}_{i,i+1}\,\Psi_4 + \mathbf{P}_{i+1}\Psi_5 \right] \otimes \Delta\boldsymbol{\rho}_i^{\perp} \right\} \frac{\mathbf{a}}{\alpha},$$

where $\mathbf{P}_i$, $\mathbf{P}_{i,i+1}$ and $\mathbf{P}_{i+1}$ are defined in (7) and

$$\Psi_3 = \frac{e^{(2)}_{(i)1,0} + 2\,(e^{(1)}_{-(i)1,-1} - e^{\alpha\,a_{i+1}})}{\alpha^{\,3}(a_i - a_{i+1})^3}, \qquad \Psi_4 = \frac{e^{(1)}_{(i)1,2} + e^{(1)}_{(i+1)1,-2}}{\alpha^{\,3}(a_i - a_{i+1})^3}, \qquad \Psi_5 = \frac{-e^{(2)}_{(i+1)1,0} - 2\,(e^{(1)}_{(i+1)1,-1} - e^{\alpha\,a_i})}{\alpha^{\,3}(a_i - a_{i+1})^3}. \tag{33}$$

On the contrary, when $a_i = a_{i+1}$, one has

$$\mathbf{J}^{(2),\exp}_{2\,\partial\Omega_{SS}} = \left\{ \frac{e^{\alpha\,a_i}}{3} \left[\mathbf{P}_i + \frac{1}{2}\,\mathbf{P}_{i,i+1} + \mathbf{P}_{i+1} \right] \otimes \Delta\boldsymbol{\rho}_i^{\perp} \right\} \frac{\mathbf{a}}{\alpha}.$$

Thus, setting

$$\mathbf{J}^{(2),\exp}_{2\,\partial\Omega_{\text{tbs}}} = \begin{cases} \mathbf{J}^{(2),\exp}_{2\,\partial\Omega_i} & \text{iff} \quad a_i \neq a_{i+1}, \\ \mathbf{J}^{(2),\exp}_{2\,\partial\Omega_{SS}} & \text{iff} \quad a_i = a_{i+1}, \end{cases}$$

one has

$$\mathbf{J}^{(2),\exp}_{2\,\Omega} = \sum_{i=1}^{n} \mathbf{J}^{(2),\exp}_{2\,\partial\Omega_{\text{tbs}}} - \mathbf{J}^{(1),\exp}_{2\,\Omega} \otimes \frac{\mathbf{a}}{\alpha} - \frac{\mathbf{a}}{\alpha} \otimes \mathbf{J}^{(1),\exp}_{2\,\Omega}, \tag{34}$$

where $\mathbf{J}^{(1),\exp}_{2\Omega}$ is supplied in (32).

5.3. Polynomial quadratic density distribution

Let us now consider a polygonal domain Ω of arbitrary shape endowed with the density distribution (10). To provide a compact representation of the ensuing results we set

$$u_i = \|\boldsymbol{\rho}_i\|^2, \qquad v_i = \boldsymbol{\rho}_i \cdot \boldsymbol{\rho}_{i+1}, \qquad w_i = \|\boldsymbol{\rho}_{i+1}\|^2,$$

and we observe that

$$\left[\tilde{\boldsymbol{\rho}}(\lambda_i) \cdot \tilde{\boldsymbol{\rho}}(\lambda_i)\right]^q = \left[u_i\,\left(1-\lambda_i\right)^2 + 2\,v_i\,\left(1-\lambda_i\right)\,\lambda_i + w_i\,\lambda_i^2 \right]^q.$$

Invoking the trinomial expansion, the previous equation becomes

$$\left[\tilde{\boldsymbol{\rho}}(\lambda_i) \cdot \tilde{\boldsymbol{\rho}}(\lambda_i)\right]^q = \sum_{r=0}^{q} \sum_{j=0}^{r} \binom{q}{r} \binom{r}{j} u_i^j\, 2^{r-j}\, v_i^{r-j}\, w_i^{q-r}\, \left(1-\lambda_i\right)^{r+j}\, \lambda_i^{2q-r-j}.$$

For its repeated use in the paper, it is also convenient to introduce the following notation

$$d_i = \binom{q}{r} \binom{r}{j} u_i^j\, v_i^{r-j}\, w_i^{q-r}\, 2^{r-j}, \qquad f^{rjb2qc}_{2qa} = \frac{(r+j+b)!\,(2\,q-r-j+c)!}{(2\,q+a)!}, \tag{35}$$

where a, b, c, j, r and q are non-negative integers.

Using the transformation (21), formula (5) and the notation defined in (7), one finally has for the integrals in (16)

$$\begin{aligned} \mathbf{J}^{(0),\text{plq}}_{2\,\Omega} &= \sum_{q=0}^{m} D^{(02)}_{2\,q} \sum_{i=1}^{n} c_i \sum_{r=0}^{q} \sum_{j=0}^{r} d_i\, f^{rj02q0}_{2q1}, \\ \mathbf{J}^{(1),\text{plq}}_{2\,\Omega} &= \sum_{q=0}^{m} D^{(12)}_{2\,q} \sum_{i=1}^{n} c_i \sum_{r=0}^{q} \sum_{j=0}^{r} d_i \left(f^{rj12q0}_{2q2}\,\boldsymbol{\rho}_i + f^{rj02q1}_{2q2}\,\boldsymbol{\rho}_{i+1} \right), \\ \mathbf{J}^{(2),\text{plq}}_{2\,\Omega} &= \sum_{q=0}^{m} D^{(22)}_{2\,q} \sum_{i=1}^{n} c_i \sum_{r=0}^{q} \sum_{j=0}^{r} d_i \left(f^{rj22q0}_{2q3}\,\mathbf{P}_i + f^{rj12q1}_{2q3}\,\mathbf{P}_{i,i+1} + f^{rj02q2}_{2q3}\,\mathbf{P}_{i+1} \right). \end{aligned} \tag{36}$$

6. Evaluation of boundary integrals for functionally graded axisymmetric polygonal solids

In this Section, we show how to evaluate analytically the boundary integrals defined in Sec. 4 in the relevant case of axisymmetric polygonal solids, i.e. solids obtained by rotating a polygonal domain around an axis of symmetry.

6.1. Polynomial density

Let us assume that the axisymmetric polygonal solid Ω is endowed with a polynomial density distribution given by (8) and that the boundary integrals $\mathbf{J}^{(0),\mathrm{pln}}_{\mathrm{ax}\,\partial\Omega}$, $\mathbf{J}^{(1),\mathrm{pln}}_{\mathrm{ax}\,\partial\Omega}$ and $\mathbf{J}^{(2),\mathrm{pln}}_{\mathrm{ax}\,\partial\Omega}$ defined in Eqs. (18) need to be computed.

Following a path of reasoning completely similar to that illustrated in Subsection 5.1, we have from (18a)

$$\mathbf{J}^{(0),\mathrm{pln}}_{\mathrm{ax}\,\partial\Omega} = P^{(2)}_{1/q} \sum_{i=1}^{n} c_i \sum_{r=0}^{q} a_i^{q-r}\, a_{i+1}^{r} \left[(q-r+1)\, b_i + (r+1)\, b_{i+1} \right], \tag{37}$$

where it has been set

$$b_i = \boldsymbol{\rho}_i \cdot \mathbf{b} \qquad b_{i+1} = \boldsymbol{\rho}_{i+1} \cdot \mathbf{b}. \tag{38}$$

Hence, on account of (17), it turns out to be

$$\mathbf{J}^{(0),\mathrm{pln}}_{\mathrm{ax}\,\Omega} = 2\pi \sum_{q=0}^{m} D^{P\,(3)}_{q} \sum_{i=1}^{n} c_i \sum_{r=0}^{q} a_i^{q-r}\, a_{i+1}^{r} \left[\prod_{q-r}^{1} b_i + \prod_{r}^{1} b_{i+1} \right]. \tag{39}$$

Analogously, the boundary integral $\mathbf{J}^{(1),\mathrm{pln}}_{\mathrm{ax}\,\partial\Omega}$ in (18b) becomes

$$\mathbf{J}^{(1),\mathrm{pln}}_{\mathrm{ax}\,\partial\Omega} = P^{(3)}_{1/q}\, \mathbf{S}^{(1),\mathrm{pln}}_{\mathrm{ax}\,\partial\Omega} = P^{(3)}_{1/q} \sum_{i=1}^{n} c_i \sum_{r=0}^{q} a_i^{q-r}\, a_{i+1}^{r} \left[\left(b_i \prod_{q-r}^{2} + b_{i+1} \prod_{q-r}^{1} \prod_{r}^{1} \right) \boldsymbol{\rho}_i + \left(b_i \prod_{q-r}^{1} \prod_{r}^{1} + b_{i+1} \prod_{r}^{2} \right) \boldsymbol{\rho}_{i+1} \right], \tag{40}$$

so that, recalling (17), the associated domain integral $\mathbf{J}^{(1),\mathrm{pln}}_{\mathrm{ax}\,\Omega}$ is given by

$$\mathbf{J}^{(1),\mathrm{pln}}_{\mathrm{ax}\,\Omega} = 2\pi \sum_{q=0}^{m} D^{P\,(4)}_{q}\, \mathbf{S}^{(1),\mathrm{pln}}_{\mathrm{ax}\,\partial\Omega}. \tag{41}$$

Finally, we infer from (18c) that

$$\begin{aligned} \mathbf{J}^{(2),\mathrm{pln}}_{\mathrm{ax}\,\partial\Omega} = P^{(4)}_{1/q}\, \mathbf{S}^{(2),\mathrm{pln}}_{\mathrm{ax}\partial\Omega} = P^{(4)}_{1/q} \sum_{i=1}^{n} c_i \sum_{r=0}^{q} a_i^{q-r}\, a_{i+1}^{r} \left[\left(b_i \prod_{q-r}^{3} + b_{i+1} \prod_{q-r}^{2} \prod_{r}^{1} \right) \mathbf{P}_i \right. \\ \left. + \left(b_i \prod_{q-r}^{2} \prod_{r}^{1} + b_{i+1} \prod_{q-r}^{1} \prod_{r}^{2} \right) \mathbf{P}_{i,i+1} + \left(b_i \prod_{q-r}^{1} \prod_{r}^{2} + b_{i+1} \prod_{r}^{3} \right) \mathbf{P}_{i+1} \right], \end{aligned} \tag{42}$$

so that formula (17) yields

$$\mathbf{J}^{(2),\mathrm{pln}}_{\mathrm{ax}\,\Omega} = 2\pi \sum_{q=0}^{m} D^{P\,(5)}_{q}\, \mathbf{S}^{(2),\mathrm{pln}}_{\mathrm{ax}\,\partial\Omega}. \tag{43}$$

6.2. Exponential density

Consider an axisymmetric polygonal solid Ω with an exponential density distribution given by equation (9). We are going to compute the boundary integrals $\mathbf{J}^{(0),\mathrm{exp}}_{\mathrm{ax}\,\Omega}$, $\mathbf{J}^{(1),\mathrm{exp}}_{\mathrm{ax}\,\Omega}$ and $\mathbf{J}^{(2),\mathrm{exp}}_{\mathrm{ax}\,\Omega}$ as defined in the formula (19). To this end, we first introduce the following notation

$$\varepsilon_{il} = b_i\, \Psi_l \qquad \varepsilon_{(i+1)l} = b_{i+1}\, \Psi_l \qquad l = 1, \dots, 9,$$

where b_i, b_{i+1} are defined in (38), $\Psi_1, \dots, \Psi_5$ are obtained from (31) and (33) while $\Psi_6, \dots, \Psi_9$ are given by:

$$\Psi_6 = \frac{e^{(3)}_{(i)1,0} - 3\, e^{(2)}_{(i)1,0} + 6\,(e^{(1)}_{(i)1,1} + e^{\alpha\, a_{i+1}})}{\alpha^4\,(a_i - a_{i+1})^4}, \qquad \Psi_7 = \frac{e^{(2)}_{(i)1,0} + 2\, e^{(1)}_{-(i)2,-3} + 2\, e^{(1)}_{-(i+1)1,3}}{\alpha^4\,(a_i - a_{i+1})^4}, \qquad \Psi_8 = \frac{e^{(2)}_{(i+1)1,0} + 2\, e^{(1)}_{(i+1)2,-3} + 2\, e^{(1)}_{(i)1,3}}{\alpha^4\,(a_i - a_{i+1})^4},$$

$$\Psi_9 = \frac{e^{(3)}_{-(i+1)1,0} - 3\, e^{(2)}_{(i+1)1,0} + 6\,(e^{\alpha\, a_i} + e^{(1)}_{-(i+1)1,1})}{\alpha^4\,(a_i - a_{i+1})^4},$$

provided that $a_i \neq a_{i+1}$.

Hence, setting

$$\mathbf{J}^{(0),\exp}_{\mathrm{ax}\,\partial\Omega_i} = (\varepsilon_{i1} + \varepsilon_{(i+1)2})\,\Delta\boldsymbol{\rho}_i^{\perp} \cdot \frac{\mathbf{a}}{\alpha} \quad \text{iff} \quad a_i \neq a_{i+1}, \qquad \mathbf{J}^{(0),\exp}_{\mathrm{ax}\,\partial\Omega_{SS}} = \frac{e^{\alpha\, a_i}}{2}\left(b_i + b_{i+1}\right)\Delta\boldsymbol{\rho}_i^{\perp} \cdot \frac{\mathbf{a}}{\alpha} \quad \text{iff} \quad a_i = a_{i+1},$$

and

$$\mathbf{J}^{(0),\exp}_{\mathrm{ax}\,\partial\Omega_{\mathrm{tbs}}} = \begin{cases} \mathbf{J}^{(0),\exp}_{\mathrm{ax}\,\partial\Omega_i} & \text{iff} \quad a_i \neq a_{i+1}, \\ \mathbf{J}^{(0),\exp}_{\mathrm{ax}\,\partial\Omega_{SS}} & \text{iff} \quad a_i = a_{i+1}, \end{cases}$$

it turns out to be

$$\mathbf{J}^{(0),\exp}_{\mathrm{ax}\,\Omega} = 2\,\pi\left[\sum_{i=1}^{n} \mathbf{J}^{(0),\exp}_{\mathrm{ax}\,\partial\Omega_{\mathrm{tbs}}} - \mathbf{J}^{(0),\exp}_{2\,\Omega}\left(\frac{\mathbf{a}}{\alpha}\cdot\mathbf{b}\right)\right], \tag{44}$$

where $\mathbf{J}^{(0),\exp}_{2\,\Omega}$ is provided by (30).

In order to evaluate $\mathbf{J}^{(1),\exp}_{\mathrm{ax}\,\Omega}$ in (19b) we preliminarily set

$$\mathbf{J}^{(1),\exp}_{\mathrm{ax}\,\partial\Omega_i} = \left\{\left[(\varepsilon_{i3} + \varepsilon_{(i+1)4})\,\boldsymbol{\rho}_i + (\varepsilon_{i4} + \varepsilon_{(i+1)5})\,\boldsymbol{\rho}_{i+1}\right] \otimes \Delta\boldsymbol{\rho}_i^{\perp}\right\}\frac{\mathbf{a}}{\alpha} \qquad \text{iff} \quad a_i \neq a_{i+1},$$

$$\mathbf{J}^{(1),\exp}_{\mathrm{ax}\,\partial\Omega_{SS}} = \left\{\frac{e^{\alpha\, a_i}}{3}\left[b_i\,\boldsymbol{\rho}_i + b_{i+1}\,\boldsymbol{\rho}_{i+1} + \frac{1}{2}\left(b_i\,\boldsymbol{\rho}_{i+1} + b_{i+1}\,\boldsymbol{\rho}_i\right)\right] \otimes \Delta\boldsymbol{\rho}_i^{\perp}\right\}\frac{\mathbf{a}}{\alpha} \qquad \text{iff} \quad a_i = a_{i+1},$$

and

$$\mathbf{J}^{(1),\exp}_{\mathrm{ax}\,\partial\Omega_{\mathrm{tbs}}} = \begin{cases} \mathbf{J}^{(1),\exp}_{\mathrm{ax}\,\partial\Omega_i} & \text{iff} \quad a_i \neq a_{i+1}, \\ \mathbf{J}^{(1),\exp}_{\mathrm{ax}\,\partial\Omega_{SS}} & \text{iff} \quad a_i = a_{i+1}. \end{cases}$$

We thus have

$$\mathbf{J}^{(1),\exp}_{\mathrm{ax}\,\Omega} = 2\,\pi\left[\sum_{i=1}^{n} \mathbf{J}^{(1),\exp}_{\mathrm{ax}\,\partial\Omega_{\mathrm{tbs}}} - \mathbf{J}^{(1),\exp}_{2\,\Omega}\left(\frac{\mathbf{a}}{\alpha}\cdot\mathbf{b}\right)\right] - \mathbf{J}^{(0),\exp}_{\mathrm{ax}\,\Omega}\frac{\mathbf{a}}{\alpha}, \tag{45}$$

where $\mathbf{J}^{(1),\exp}_{2\,\Omega}$ and $\mathbf{J}^{(0),\exp}_{\mathrm{ax}\,\Omega}$ are given by (32) and (44) respectively.

It is also useful to introduce the following notation

$$\mathbf{A}_i = \varepsilon_{i6}\,\mathbf{P}_i + \varepsilon_{i7}\,\mathbf{P}_{i,i+1} + \varepsilon_{i8}\,\mathbf{P}_{i+1}, \qquad \mathbf{B}_i = \varepsilon_{(i+1)7}\,\mathbf{P}_i + \varepsilon_{(i+1)8}\,\mathbf{P}_{i,i+1} + \varepsilon_{(i+1)9}\,\mathbf{P}_{i+1}, \qquad \mathbf{C}_i = \frac{e^{\alpha\, a_i}}{4}\,b_i\left(\mathbf{P}_i + \frac{1}{3}\,\mathbf{P}_{i,i+1} + \frac{1}{3}\,\mathbf{P}_{i+1}\right),$$

$$\mathbf{D}_i = \frac{e^{\alpha\, a_i}}{4}\,b_{i+1}\left(\frac{1}{3}\,\mathbf{P}_i + \frac{1}{3}\,\mathbf{P}_{i,i+1} + \mathbf{P}_{i+1}\right).$$

Hence, setting

$$\mathbf{J}^{(2),\exp}_{\mathrm{ax}\,\partial\Omega_i} = \left[\left(\mathbf{A}_i + \mathbf{B}_i\right) \otimes \Delta\boldsymbol{\rho}_i^{\perp}\right]\frac{\mathbf{a}}{\alpha}, \qquad \mathbf{J}^{(2),\exp}_{\mathrm{ax}\,\partial\Omega_{SS}} = \left[\left(\mathbf{C}_i + \mathbf{D}_i\right) \otimes \Delta\boldsymbol{\rho}_i^{\perp}\right]\frac{\mathbf{a}}{\alpha},$$

$$\mathbf{J}^{(2),\exp}_{\mathrm{ax}\,\partial\Omega_{\mathrm{tbs}}} = \begin{cases} \mathbf{J}^{(2),\exp}_{\mathrm{ax}\,\partial\Omega_i} & \text{iff} \quad a_i \neq a_{i+1}, \\ \mathbf{J}^{(2),\exp}_{\mathrm{ax}\,\partial\Omega_{SS}} & \text{iff} \quad a_i = a_{i+1}, \end{cases}$$

one finally arrives at

$$\mathbf{J}^{(2),\exp}_{\mathrm{ax}\,\Omega} = 2\,\pi\left[\sum_{i=1}^{n} \mathbf{J}^{(2),\exp}_{\mathrm{ax}\,\partial\Omega_{\mathrm{tbs}}} - \mathbf{J}^{(2),\exp}_{2\,\Omega}\left(\frac{\mathbf{a}}{\alpha}\cdot\mathbf{b}\right)\right] - \left(\mathbf{J}^{(1),\exp}_{\mathrm{ax}\,\Omega} \otimes \frac{\mathbf{a}}{\alpha} + \frac{\mathbf{a}}{\alpha} \otimes \mathbf{J}^{(1),\exp}_{\mathrm{ax}\,\Omega}\right), \tag{46}$$

where $\mathbf{J}^{(2),\exp}_{2\,\Omega}$ and $\mathbf{J}^{(1),\exp}_{\mathrm{ax}\,\Omega}$ are provided by (34) and (45) respectively.

6.3. Polynomial quadratic density distribution

In the case of axisymmetric solids with a polynomial quadratic density distribution as defined in equation (10) one has, recalling (20)

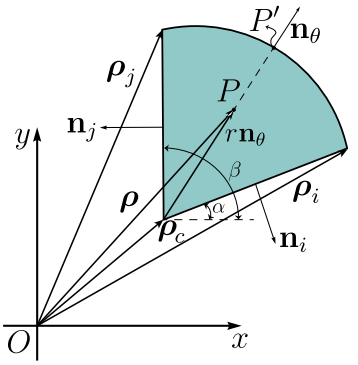

Fig. 2. A circular sector.

$$
\begin{aligned}
\mathbf{J}_{\mathrm{ax}\,\Omega}^{(0),\mathrm{plq}} &= 2\,\pi \sum_{q=0}^{m} D_{2\,q}^{(03)} \sum_{i=1}^{n} c_i \sum_{r=0}^{q} \sum_{j=0}^{r} d_i \left[f_{2q2}^{rj12q0}\, b_i + f_{2q2}^{rj02q1}\, b_{i+1} \right], \\
\mathbf{J}_{\mathrm{ax}\,\Omega}^{(1),\mathrm{plq}} &= 2\,\pi \sum_{q=0}^{m} D_{2\,q}^{(13)} \sum_{i=1}^{n} c_i \sum_{r=0}^{q} \sum_{j=0}^{r} d_i \left\{ \left[f_{2q3}^{rj22q0}\, b_i + f_{2q3}^{rj12q1}\, b_{i+1} \right] \boldsymbol{\rho}_i + \left[f_{2q3}^{rj12q1}\, b_i + f_{2q3}^{rj02q2}\, b_{i+1} \right] \boldsymbol{\rho}_{i+1} \right\}, \\
\mathbf{J}_{\mathrm{ax}\,\Omega}^{(2),\mathrm{plq}} &= 2\,\pi \sum_{q=0}^{m} D_{2\,q}^{(23)} \sum_{i=1}^{n} c_i \sum_{r=0}^{q} \sum_{j=0}^{r} d_i \left\{ \left[f_{2q4}^{rj32q0}\, b_i + f_{2q4}^{rj22q1}\, b_{i+1} \right] \mathbf{P}_i + \left[f_{2q4}^{rj22q1}\, b_i + f_{2q4}^{rj12q2}\, b_{i+1} \right] \mathbf{P}_{i,i+1} \right. \\
&\quad \left. + \left[f_{2q4}^{rj12q2}\, b_i + f_{2q4}^{rj02q3}\, b_{i+1} \right] \mathbf{P}_{i+1} \right\},
\end{aligned}
\tag{47}
$$

where the constants c_i and d_i are defined in (7) and (35), respectively, while b_i and b_{i+1} in (38).

7. Functionally graded circular sectors

Let $\diamondsuit$ be a domain having the shape of a circular sector of radius R and amplitude $\beta - \alpha$, see, e.g., Fig. 2. The centre C of the circle from which $\diamondsuit$ is extracted is identified by the position vector $\boldsymbol{\rho}_C$, whereas the starting and ending points of the arc are located by the position vectors designated as $\boldsymbol{\rho}_i$ and $\boldsymbol{\rho}_j$, respectively.

Therefore, a generic point P belonging to $\diamondsuit$ is identified by the position vector

$$
\boldsymbol{\rho} = \boldsymbol{\rho}_C + r\,\mathbf{n}_\theta, \quad r \in [0, R], \tag{48}
$$

where $\mathbf{n}_\theta = [\cos\theta \;\; \sin\theta]^T$ and $\theta \in [\alpha, \beta]$.

We are interested to express the mass moments (1) by means of boundary integrals for density varying along the radial direction from $\boldsymbol{\rho}_C$. Specifically, we shall consider

- a linear density distribution

$$
\varrho^{\mathrm{lin}}(\boldsymbol{\rho}) = \|\boldsymbol{\rho} - \boldsymbol{\rho}_C\| = \|\Delta\boldsymbol{\rho}_C\|, \tag{49}
$$

- a quadratic density distribution

$$
\varrho^{\mathrm{qua}}(\boldsymbol{\rho}) = \|\Delta\boldsymbol{\rho}_C\|^2. \tag{50}
$$

In particular, by applying Gauss theorem, we shall derive analytical formulas for the mass moments of functionally graded circular sectors depending upon the anomalies of the segments defining the sector and the coordinates of the relevant endpoints.

The derivation of such formulas requires, as an intermediate step, the knowledge of the mass moments referred to homogeneous circular sectors. For this reason, they are explicitly computed in the next subsection.

7.1. Mass moments of homogeneous circular sectors

Invoking (4a) one has

$$
A_{\diamondsuit} = \frac{1}{2} \int_{\partial\diamondsuit} \boldsymbol{\rho} \cdot \mathbf{n}\, \mathrm{d}s = \frac{1}{2} \Big[\int_{ssi} \boldsymbol{\rho} \cdot \mathbf{n}\, \mathrm{d}s + \int_{\partial\diamondsuit_i} \boldsymbol{\rho} \cdot \mathbf{n}_\theta\, \mathrm{d}s + \int_{ssj} \boldsymbol{\rho} \cdot \mathbf{n}\, \mathrm{d}s \Big],
$$

where ssi (ssj) denotes the side of the circular sector connecting C and the vertex i (j) while $\partial\diamondsuit_i$ is the arc connecting the vertices i and j.

Denoting by λ_m the parameter describing the generic point along the sides ssi and ssj, i.e. $\tilde{\boldsymbol{\rho}}(\lambda_m) = \boldsymbol{\rho}_C + \lambda_m(\boldsymbol{\rho}_m - \boldsymbol{\rho}_C)$, $m = i\ (j)$, the first and third integral in the formula above are given by

$$\int_{ssm} \boldsymbol{\rho}\cdot\mathbf{n}\,\mathrm{d}s = \int_0^1 \tilde{\boldsymbol{\rho}}(\lambda_m)\cdot\mathbf{n}_m\,\mathrm{d}\lambda_m\,R = R\,\boldsymbol{\rho}_C\cdot\mathbf{n}_m$$

where $\mathbf{n}_m$ is the unit normal to the side ssm, $m = i, j$.

Furthermore, it turns out to be

$$\boldsymbol{\rho}_\theta = \boldsymbol{\rho}_C + R\,\mathbf{n}_\theta \qquad \|\boldsymbol{\rho} - \boldsymbol{\rho}_C\| = R \qquad \mathrm{d}s = R\,\mathrm{d}\theta, \tag{51}$$

along the arc $\partial\diamondsuit_i$; hence, denoting by $\mathbf{N}^{(1)}_{\theta\diamondsuit}$ the integral of $\mathbf{n}_\theta$ along the arc, a quantity evaluated in formula (D.1) of the SM 4, one has

$$A_\diamondsuit = \frac{R}{2}\Big[\int_\alpha^\beta \boldsymbol{\rho}_C\cdot\mathbf{n}_\theta\,\mathrm{d}\theta + R\int_\alpha^\beta \mathrm{d}\theta + \int_0^1 \tilde{\boldsymbol{\rho}}(\lambda_i)\cdot\mathbf{n}_i\,\mathrm{d}\lambda_i + \int_0^1 \tilde{\boldsymbol{\rho}}(\lambda_j)\cdot\mathbf{n}_j\,\mathrm{d}\lambda_j\Big] = \frac{R}{2}\left[R(\beta-\alpha) + \boldsymbol{\rho}_C\cdot\left(\mathbf{N}^{(1)}_{\theta\diamondsuit} + \mathbf{n}_i + \mathbf{n}_j\right)\right] = \frac{R^2}{2}(\beta-\alpha),$$

since it is easy to show that $\mathbf{N}^{(1)}_{\theta\diamondsuit} + \mathbf{n}_i + \mathbf{n}_j = \mathbf{o}$ where $\mathbf{o}$ is the null vector.

Analogously, introducing the notation

$$n_{s\boldsymbol{\rho}} = \boldsymbol{\rho}\cdot\mathbf{n}_s, \quad n_{Cs\boldsymbol{\rho}} = \boldsymbol{\rho}_C\cdot\mathbf{n}_s \qquad s = i, j, \theta, \tag{52}$$

one has from formula (4b)

$$\begin{aligned}
\mathbf{s}_\diamondsuit &= \frac{1}{3}\int_{\partial\diamondsuit}(\boldsymbol{\rho}\cdot\mathbf{n})\,\boldsymbol{\rho}\,\mathrm{d}s = \frac{1}{3}\Big[\int_{ssi} n_{i\boldsymbol{\rho}}\,\boldsymbol{\rho}\,\mathrm{d}s + \int_{\partial\diamondsuit_i} n_{\theta\boldsymbol{\rho}}\,\boldsymbol{\rho}_\theta\,\mathrm{d}s + \int_{ssj} n_{j\boldsymbol{\rho}}\,\boldsymbol{\rho}\,\mathrm{d}s\Big] = \\
&= \frac{R}{3}\Big[\int_\alpha^\beta (n_{C\theta\boldsymbol{\rho}} + R)\,\boldsymbol{\rho}_\theta\,\mathrm{d}\theta + \int_0^1 n_{Ci\boldsymbol{\rho}}\,\tilde{\boldsymbol{\rho}}(\lambda_i)\,\mathrm{d}\lambda_i + \int_0^1 n_{Cj\boldsymbol{\rho}}\,\tilde{\boldsymbol{\rho}}(\lambda_j)\,\mathrm{d}\lambda_j\Big] = \\
&= \frac{R}{3}\Big\{R(\beta-\alpha)\,\boldsymbol{\rho}_C + R\,\mathbf{N}^{(2)}_{\theta\diamondsuit}\,\boldsymbol{\rho}_C + R^2\,\mathbf{N}^{(1)}_{\theta\diamondsuit} + \frac{1}{2}\left[n_{Ci\boldsymbol{\rho}}\,\Delta\boldsymbol{\rho}_{iC} + n_{Cj\boldsymbol{\rho}}\,\Delta\boldsymbol{\rho}_{jC}\right]\Big\},
\end{aligned} \tag{53}$$

where the rank-two tensor $\mathbf{N}^{(2)}_{\theta\diamondsuit}$ is reported in the formula (D.2) of the SM 4 and it has been set

$$\Delta\boldsymbol{\rho}_{mC} = \left(\boldsymbol{\rho}_m - \boldsymbol{\rho}_C\right) \qquad m = i, j. \tag{54}$$

Finally, setting

$$\begin{aligned}
\boldsymbol{\rho}^{(2)}_s &= n_{s\boldsymbol{\rho}}\,\boldsymbol{\rho}\otimes\boldsymbol{\rho} && s = i, j, \theta, \\
\mathbf{P}_{mC} &= \boldsymbol{\rho}_C\otimes\Delta\boldsymbol{\rho}_{mC} + \Delta\boldsymbol{\rho}_{mC}\otimes\boldsymbol{\rho}_C && m = i, j, \\
\mathbf{N}^{(2)}_{mc} &= n_{Cm\boldsymbol{\rho}}\left[\frac{1}{2}\mathbf{P}_{mC} + \frac{1}{3}\Delta\boldsymbol{\rho}_{mC}\otimes\Delta\boldsymbol{\rho}_{mC}\right] && m = i, j,
\end{aligned}$$

formula (4c) yields

$$\begin{aligned}
\mathbf{J}_\diamondsuit &= \frac{1}{4}\int_{\partial\diamondsuit}(\boldsymbol{\rho}\cdot\mathbf{n})\,(\boldsymbol{\rho}\otimes\boldsymbol{\rho})\,\mathrm{d}s = \frac{1}{4}\Big[\int_{ssi}\boldsymbol{\rho}^{(2)}_i\,\mathrm{d}s + \int_{\partial\diamondsuit_i}\boldsymbol{\rho}^{(2)}_\theta\,\mathrm{d}s + \int_{ssj}\boldsymbol{\rho}^{(2)}_j\,\mathrm{d}s\Big] = \\
&= \frac{R}{4}\Big[\int_\alpha^\beta (n_{C\theta\boldsymbol{\rho}} + R)(\boldsymbol{\rho}_\theta\otimes\boldsymbol{\rho}_\theta)\,\mathrm{d}\theta + \int_0^1 n_{Ci\boldsymbol{\rho}}\,(\tilde{\boldsymbol{\rho}}(\lambda_i)\otimes\tilde{\boldsymbol{\rho}}(\lambda_i))\,\mathrm{d}\lambda_i + \int_0^1 n_{Cj\boldsymbol{\rho}}\,(\tilde{\boldsymbol{\rho}}(\lambda_j)\otimes\tilde{\boldsymbol{\rho}}(\lambda_j))\,\mathrm{d}\lambda_j\Big],
\end{aligned} \tag{55}$$

so that one has

$$\mathbf{J}_\diamondsuit = \frac{R}{4}\Big[R(\beta-\alpha)\,\left(\boldsymbol{\rho}_C\otimes\boldsymbol{\rho}_C\right) + R(\boldsymbol{\rho}_C\cdot\mathbf{N}^{(1)}_{\theta\diamondsuit} + R)\,\left(\boldsymbol{\rho}_C\otimes\mathbf{N}^{(1)}_{\theta\diamondsuit} + \mathbf{N}^{(1)}_{\theta\diamondsuit}\otimes\boldsymbol{\rho}_C\right) + R^2\,\mathbf{N}^{(3)}_{\theta\diamondsuit}\,\boldsymbol{\rho}_C + R^3\,\mathbf{N}^{(2)}_{\theta\diamondsuit} + \mathbf{N}^{(2)}_{ic} + \mathbf{N}^{(2)}_{jc}\Big],$$

where the expression of the rank-three tensor $\mathbf{N}^{(3)}_{\theta\diamondsuit}$ can be found in the formula (D.3) of the SM 4.

7.2. Radially linear density distribution

In this case we need to evaluate the integrals

$$\mathbf{J}_{2\diamondsuit}^{(0),\mathrm{lin}} = \int_{\diamondsuit} \|\Delta\boldsymbol{\rho}_C\| \,\mathrm{d}A,$$
$$\mathbf{J}_{2\diamondsuit}^{(1),\mathrm{lin}} = \int_{\diamondsuit} \|\Delta\boldsymbol{\rho}_C\| \,\boldsymbol{\rho}\,\mathrm{d}A,$$
$$\mathbf{J}_{2\diamondsuit}^{(2),\mathrm{lin}} = \int_{\diamondsuit} \|\Delta\boldsymbol{\rho}_C\| \,(\boldsymbol{\rho}\otimes\boldsymbol{\rho})\,\mathrm{d}A;$$

to get the result we shall replace $\boldsymbol{\rho}$ by $\Delta\boldsymbol{\rho}_C + \boldsymbol{\rho}_C$ in the evaluation of the $\mathbf{J}_{2\diamondsuit}^{(1),\mathrm{lin}}$ and $\mathbf{J}_{2\diamondsuit}^{(2),\mathrm{lin}}$.

Upon specialisation of the differential identity (E.5) in the SM 5 one has

$$\mathbf{J}_{2\diamondsuit}^{(0),\mathrm{lin}} = \frac{1}{3}\int_{\partial\diamondsuit} \|\Delta\boldsymbol{\rho}_C\|\,\Delta\boldsymbol{\rho}_C\cdot\mathbf{n}\,\mathrm{d}s = \frac{R}{3}\int_{\partial\diamondsuit_i} \Delta\boldsymbol{\rho}_C\cdot\mathbf{n}_\theta\,R\,\mathrm{d}\theta = \frac{R^2}{3}\int_\alpha^\beta R\,\mathrm{d}\theta = \frac{R^3}{3}(\beta-\alpha), \tag{56}$$

since $\Delta\boldsymbol{\rho}_C\cdot\mathbf{n}=0$ along the sides ssi and ssj.

The mass moment $\mathbf{J}_{2\diamondsuit}^{(1),\mathrm{lin}}$ can also be written in the following way

$$\mathbf{J}_{2\diamondsuit}^{(1),\mathrm{lin}} = \int_{\diamondsuit} \|\Delta\boldsymbol{\rho}_C\|\,\Delta\boldsymbol{\rho}_C\,\mathrm{d}A + \boldsymbol{\rho}_C\,\mathbf{J}_{2\diamondsuit}^{(0),\mathrm{lin}} = \mathbf{c}_\diamondsuit + \boldsymbol{\rho}_C\,\mathbf{J}_{2\diamondsuit}^{(0),\mathrm{lin}}, \tag{57}$$

so that one infers from the identity (E.5), specialised to the case $k=1$, that

$$\mathbf{c}_\diamondsuit = \frac{1}{4}\int_{\partial\diamondsuit} \|\Delta\boldsymbol{\rho}_C\|\,[\otimes\Delta\boldsymbol{\rho}_C,\,2]\,\mathbf{n}\,\mathrm{d}s = \frac{1}{4}\int_{\partial\diamondsuit_i} \|\Delta\boldsymbol{\rho}_C\|\,[\otimes\Delta\boldsymbol{\rho}_C,\,2]\,\mathbf{n}_\theta\,\mathrm{d}s = \frac{R^4}{4}\int_\alpha^\beta \mathbf{n}_\theta\,\mathrm{d}\theta = \frac{R^4}{4}\mathbf{N}_{\theta\diamondsuit}^{(1)}. \tag{58}$$

Analogously, one has

$$\mathbf{J}_{2\diamondsuit}^{(2),\mathrm{lin}} = \mathbf{C}_\diamondsuit + \boldsymbol{\rho}_C\otimes\mathbf{c}_\diamondsuit + \mathbf{c}_\diamondsuit\otimes\boldsymbol{\rho}_C + \left(\boldsymbol{\rho}_C\otimes\boldsymbol{\rho}_C\right)\mathbf{J}_{2\diamondsuit}^{(0),\mathrm{lin}}, \tag{59}$$

where one infers from the identity (E.5) for $k=2$ that

$$\begin{aligned}\mathbf{C}_\diamondsuit &= \int_{\diamondsuit} \|\Delta\boldsymbol{\rho}_C\|\,[\otimes\Delta\boldsymbol{\rho}_C,\,2]\,\mathrm{d}A = \frac{1}{5}\int_{\partial\diamondsuit} \|\Delta\boldsymbol{\rho}_C\|\,\left[\otimes\Delta\boldsymbol{\rho}_C,\,3\right]\,\mathbf{n}\,\mathrm{d}s = \frac{1}{5}\int_{\partial\diamondsuit_i} \|\Delta\boldsymbol{\rho}_C\|\,\left[\otimes\Delta\boldsymbol{\rho}_C,\,3\right]\,\mathbf{n}_\theta\,\mathrm{d}s = \frac{R^5}{5}\int_\alpha^\beta \mathbf{n}_\theta\otimes\mathbf{n}_\theta\,\mathrm{d}\theta = \\ &= \frac{R^5}{5}\mathbf{N}_{\theta\diamondsuit}^{(2)}.\end{aligned} \tag{60}$$

7.3. Radially quadratic density distribution

Recalling (50) the following integrals are required

$$\mathbf{J}_{2\diamondsuit}^{(0),\mathrm{qua}} = \int_{\diamondsuit} \|\Delta\boldsymbol{\rho}_C\|^2\,\mathrm{d}A,$$
$$\mathbf{J}_{2\diamondsuit}^{(1),\mathrm{qua}} = \int_{\diamondsuit} \|\Delta\boldsymbol{\rho}_C\|^2\,\boldsymbol{\rho}\,\mathrm{d}A,$$
$$\mathbf{J}_{2\diamondsuit}^{(2),\mathrm{qua}} = \int_{\diamondsuit} \|\Delta\boldsymbol{\rho}_C\|^2\,(\boldsymbol{\rho}\otimes\boldsymbol{\rho})\,\mathrm{d}A.$$

By using the differential identity (E.6) and applying Gauss theorem, one arrives at

$$\mathbf{J}_{2\diamondsuit}^{(0),\mathrm{qua}} = \frac{1}{4}\int_{\partial\diamondsuit} \|\Delta\boldsymbol{\rho}_C\|^2\,n_{\Delta\rho_C}\,\mathrm{d}s = \frac{1}{4}\int_\alpha^\beta R^4\,\mathrm{d}\theta = \frac{R^4}{4}(\beta-\alpha), \tag{61}$$

while the differential identity (E.6) yields, for $k=1$

$$\mathbf{J}^{(1),\mathrm{qua}}_{2\diamond} = \frac{1}{5}\int_{\partial\diamond} \|\Delta\rho_C\|^2\,\Delta\rho_C\,n_{\Delta\rho_C}\,\mathrm{d}s + \int_{\diamond} \|\Delta\rho_C\|^2\,\rho_C\,\mathrm{d}A = \frac{R^5}{5}\,\mathbf{N}^{(1)}_{\theta\diamond} + \mathbf{J}^{(0),\mathrm{qua}}_{2\diamond}\,\rho_C, \tag{62}$$

in which the expression of $\mathbf{N}^{(1)}_{\theta\diamond}$ is provided by Eq. (D.1) and that of $\mathbf{J}^{(0),\mathrm{qua}}_{2\diamond}$ by Eq. (61).

Finally, by using the differential identity (E.6) for $k=2$, the following expression is obtained

$$\begin{aligned}\mathbf{J}^{(2),\mathrm{qua}}_{2\diamond} &= \frac{1}{6}\int_{\partial\diamond} \|\Delta\rho_C\|^2\,[\otimes\Delta\rho_C,\,2]\,n_{\Delta\rho_C}\,\mathrm{d}s + \mathbf{J}^{(1),\mathrm{qua}}_{2\diamond}\otimes\rho_C + \rho_C\otimes\mathbf{J}^{(1),\mathrm{qua}}_{2\diamond} - \mathbf{J}^{(0),\mathrm{qua}}_{2\diamond}\,(\rho_C\otimes\rho_C) = \\ &= \frac{R^6}{6}\,\mathbf{N}^{(2)}_{\theta\diamond} + \mathbf{J}^{(1),\mathrm{qua}}_{2\diamond}\otimes\rho_C + \rho_C\otimes\mathbf{J}^{(1),\mathrm{qua}}_{2\diamond} - \mathbf{J}^{(0),\mathrm{qua}}_{2\diamond}\,(\rho_C\otimes\rho_C),\end{aligned} \tag{63}$$

where $\mathbf{N}^{(2)}_{\theta\diamond}$ is reported in Eq. (D.2) while $\mathbf{J}^{(0),\mathrm{qua}}_{2\diamond}$ and $\mathbf{J}^{(1),\mathrm{qua}}_{2\diamond}$ are provided by Eqs. (61) and (62), respectively.

8. Functionally graded axisymmetric circular solids

Let us now consider axisymmetric solids obtained by rotating circular sectors around an axis of symmetry. A linear or quadratic variation of density along the radial direction starting from ρ_C is assumed.

8.1. Radially linear density distribution

Recalling formula (2) and the expression (49), we are now led to computing the following integrals

$$\mathbf{J}^{(0),\mathrm{lin}}_{\mathrm{ax}\diamond} = 2\pi\int_{\diamond} \|\Delta\rho_C\|\,(\boldsymbol{\rho}\cdot\mathbf{b})\,\mathrm{d}A, \tag{64a}$$

$$\mathbf{J}^{(1),\mathrm{lin}}_{\mathrm{ax}\diamond} = 2\pi\int_{\diamond} \|\Delta\rho_C\|\,(\boldsymbol{\rho}\cdot\mathbf{b})\,\boldsymbol{\rho}\,\mathrm{d}A, \tag{64b}$$

$$\mathbf{J}^{(2),\mathrm{lin}}_{\mathrm{ax}\diamond} = 2\pi\int_{\diamond} \|\Delta\rho_C\|\,(\boldsymbol{\rho}\cdot\mathbf{b})\,(\boldsymbol{\rho}\otimes\boldsymbol{\rho})\,\mathrm{d}A. \tag{64c}$$

Setting

$$n_{\Delta\rho_C} = \Delta\rho_C\cdot\mathbf{n}, \qquad n_{\theta\Delta\rho_C} = \Delta\rho_C\cdot\mathbf{n}_\theta,$$

the differential identity (F.1) of the SM 5 yields

$$\mathbf{J}^{(0),\mathrm{lin}}_{\mathrm{ax}\diamond} = \frac{2\pi}{3}\int_{\partial\diamond} \|\Delta\rho_C\|\,(\boldsymbol{\rho}\cdot\mathbf{b})\,n_{\Delta\rho_C}\,\mathrm{d}s - \frac{2\pi}{3}\,\mathbf{c}_\diamond\cdot\mathbf{b} = \frac{2\pi}{3}\int_{\partial\diamond_i} \|\Delta\rho_C\|\,\left(\boldsymbol{\rho}_\theta\cdot\mathbf{b}\right)\,n_{\theta\Delta\rho_C}\,\mathrm{d}s - \frac{2\pi}{3}\,\mathbf{c}_\diamond\cdot\mathbf{b},$$

where the expression of $\mathbf{c}_\diamond$ is reported in Eq. (58).

Hence, by invoking Eq. (51), one finally arrives at

$$\mathbf{J}^{(0),\mathrm{lin}}_{\mathrm{ax}\diamond} = 2\pi\left[\frac{R^3}{3}\left(\boldsymbol{\rho}_C\cdot\mathbf{b}\right)(\beta-\alpha) + \frac{R^4}{4}\left(\mathbf{N}^{(1)}_{\theta\diamond}\cdot\mathbf{b}\right)\right], \tag{65}$$

in which $\mathbf{N}^{(1)}_{\theta\diamond}$ is provided in Eq. (D.1).

To compute $\mathbf{J}^{(1),\mathrm{lin}}_{\mathrm{ax}\diamond}$ we notice that its expression in Eq. (64b) is amenable to the following equivalent form

$$\mathbf{J}^{(1),\mathrm{lin}}_{\mathrm{ax}\diamond} = 2\pi\int_{\diamond} \|\Delta\rho_C\|\,(\boldsymbol{\rho}\cdot\mathbf{b})\,\mathrm{d}A\,\rho_C + 2\pi\int_{\diamond} \|\Delta\rho_C\|\,(\boldsymbol{\rho}\cdot\mathbf{b})\,\Delta\rho_C\,\mathrm{d}A = \mathbf{J}^{(0),\mathrm{lin}}_{\mathrm{ax}\diamond}\,\rho_C + 2\pi\int_{\diamond} \|\Delta\rho_C\|\,(\boldsymbol{\rho}\cdot\mathbf{b})\,\Delta\rho_C\,\mathrm{d}A,$$

where $\mathbf{J}^{(0),\mathrm{lin}}_{\mathrm{ax}\diamond}$ is evaluated in Eq. (65).

Using the differential identity (F.2) to transform the last integral in the previous equation, one obtains

$$\begin{aligned}\mathbf{J}^{(1),\mathrm{lin}}_{\mathrm{ax}\diamond} &= \frac{2\pi}{4}\int_{\partial\diamond} \|\Delta\rho_C\|\,(\boldsymbol{\rho}\cdot\mathbf{b})\,\left[\otimes\Delta\rho_C,\,2\right]\,\mathbf{n}\,\mathrm{d}s - \frac{2\pi}{4}\left[\int_{\diamond} \|\Delta\rho_C\|\,\left[\otimes\Delta\rho_C,\,2\right]\,\mathrm{d}A\right]\mathbf{b} + \mathbf{J}^{(0),\mathrm{lin}}_{\mathrm{ax}\diamond}\,\rho_C = \\ &= \frac{\pi}{2}\int_{\partial\diamond_i} \|\Delta\rho_C\|\,\left(\boldsymbol{\rho}_\theta\cdot\mathbf{b}\right)\left[\otimes\Delta\rho_C,\,2\right]\,\mathbf{n}_\theta\,\mathrm{d}s - \frac{\pi}{2}\,\mathbf{C}_\diamond\,\mathbf{b} + \mathbf{J}^{(0),\mathrm{lin}}_{\mathrm{ax}\diamond}\,\rho_C,\end{aligned}$$

in which the tensor $\mathbf{C}_\diamond$ is defined in Eq. (60).

Finally, by virtue of Eq. (51), one arrives at

$$\mathbf{J}^{(1),\mathrm{lin}}_{\mathrm{ax}\diamondsuit} = 2\pi \left[\frac{R^4}{4} \left(\boldsymbol{\rho}_C \cdot \mathbf{b}\right) \mathbf{N}^{(1)}_{\theta\diamondsuit} + \frac{R^5}{5} \mathbf{N}^{(2)}_{\theta\diamondsuit} \mathbf{b} \right] + \mathbf{J}^{(0),\mathrm{lin}}_{\mathrm{ax}\diamondsuit} \boldsymbol{\rho}_C, \tag{66}$$

where the order two tensor $\mathbf{N}^{(2)}_{\theta\diamondsuit}$ is given by Eq. (D.2).

To evaluate $\mathbf{J}^{(2),\mathrm{lin}}_{\mathrm{ax}\diamondsuit}$ it is convenient to set

$$\mathbf{J}_{\mathrm{Gax}} = \boldsymbol{\rho}_C \otimes \mathbf{J}^{(1),\mathrm{lin}}_{\mathrm{ax}\diamondsuit} + \mathbf{J}^{(1),\mathrm{lin}}_{\mathrm{ax}\diamondsuit} \otimes \boldsymbol{\rho}_C - \mathbf{J}^{(0),\mathrm{lin}}_{\mathrm{ax}\diamondsuit} \left(\boldsymbol{\rho}_C \otimes \boldsymbol{\rho}_C\right),$$

so that application of the differential identity (F.3) yields

$$\begin{aligned}
\mathbf{J}^{(2),\mathrm{lin}}_{\mathrm{ax}\diamondsuit} &= 2\pi \int_{\diamondsuit} \|\Delta\boldsymbol{\rho}_C\| \left(\boldsymbol{\rho} \cdot \mathbf{b}\right) \left[\otimes \Delta\boldsymbol{\rho}_C,\, 2\right] \mathrm{d}A + \boldsymbol{\rho}_C \otimes \left(\mathbf{J}^{(1),\mathrm{lin}}_{\mathrm{ax}\diamondsuit} - \mathbf{J}^{(0),\mathrm{lin}}_{\mathrm{ax}\diamondsuit} \boldsymbol{\rho}_C\right) + \left(\mathbf{J}^{(1),\mathrm{lin}}_{\mathrm{ax}\diamondsuit} - \mathbf{J}^{(0),\mathrm{lin}}_{\mathrm{ax}\diamondsuit} \boldsymbol{\rho}_C\right) \otimes \boldsymbol{\rho}_C + \mathbf{J}^{(0),\mathrm{lin}}_{\mathrm{ax}\diamondsuit} \left(\boldsymbol{\rho}_C \otimes \boldsymbol{\rho}_C\right) = \\
&= \frac{2\pi}{5} \int_{\partial\diamondsuit} \|\Delta\boldsymbol{\rho}_C\| \left(\boldsymbol{\rho} \cdot \mathbf{b}\right) \left[\otimes \Delta\boldsymbol{\rho}_C,\, 3\right] \mathbf{n}\, \mathrm{d}s - \frac{2\pi}{5} \left[\int_{\diamondsuit} \|\Delta\boldsymbol{\rho}_C\| \left(\boldsymbol{\rho} \cdot \mathbf{b}\right) \left[\otimes \Delta\boldsymbol{\rho}_C,\, 3\right] \mathrm{d}A \right] \mathbf{b} + \mathbf{J}_{\mathrm{Gax}} = \\
&= \frac{2\pi}{5} \int_{\partial\diamondsuit_i} \|\Delta\boldsymbol{\rho}_C\| \left(\boldsymbol{\rho}_\theta \cdot \mathbf{b}\right) \left[\otimes \Delta\boldsymbol{\rho}_C,\, 2\right] n_{\theta\Delta\boldsymbol{\rho}_C}\, \mathrm{d}s - \frac{\pi}{15} \left[\int_{\partial\diamondsuit} \|\Delta\boldsymbol{\rho}_C\| \left[\otimes \Delta\boldsymbol{\rho}_C,\, 4\right] \mathbf{n}\, \mathrm{d}s \right] \mathbf{b} + \mathbf{J}_{\mathrm{Gax}},
\end{aligned}$$

where $\mathbf{J}^{(0),\mathrm{lin}}_{\mathrm{ax}\diamondsuit}$, $\mathbf{J}^{(1),\mathrm{lin}}_{\mathrm{ax}\diamondsuit}$ have been computed in Eqs. (65), (66) and use has been made of the differential identity (E.5).

Finally, by invoking Eqs. (48) and (51) one arrives at

$$\mathbf{J}^{(2),\mathrm{lin}}_{\mathrm{ax}\diamondsuit} = 2\pi \left[\frac{R^5}{5} \left(\boldsymbol{\rho}_C \cdot \mathbf{b}\right) \mathbf{N}^{(2)}_{\theta\diamondsuit} + \frac{R^6}{6} \mathbf{N}^{(3)}_{\theta\diamondsuit} \mathbf{b} \right] + \mathbf{J}_{\mathrm{Gax}}, \tag{67}$$

where $\mathbf{N}^{(3)}_{\theta\diamondsuit}$ is an order three tensor whose matrix representation can be found in Eq. (D.3).

8.2. Radially quadratic density distribution

In this case, based on (50), the following integrals are needed:

$$\begin{aligned}
\mathbf{J}^{(0),\mathrm{qua}}_{\mathrm{ax}\diamondsuit} &= 2\pi \int_{\diamondsuit} \|\Delta\boldsymbol{\rho}_C\|^2 \left(\boldsymbol{\rho} \cdot \mathbf{b}\right) \mathrm{d}A, \\
\mathbf{J}^{(1),\mathrm{qua}}_{\mathrm{ax}\diamondsuit} &= 2\pi \int_{\diamondsuit} \|\Delta\boldsymbol{\rho}_C\|^2 \left(\boldsymbol{\rho} \cdot \mathbf{b}\right) \boldsymbol{\rho}\, \mathrm{d}A, \\
\mathbf{J}^{(2),\mathrm{qua}}_{\mathrm{ax}\diamondsuit} &= 2\pi \int_{\diamondsuit} \|\Delta\boldsymbol{\rho}_C\|^2 \left(\boldsymbol{\rho} \cdot \mathbf{b}\right) \left(\boldsymbol{\rho} \otimes \boldsymbol{\rho}\right) \mathrm{d}A.
\end{aligned}$$

By virtue Eq. (F.4), one has

$$\mathbf{J}^{(0),\mathrm{qua}}_{\mathrm{ax}\diamondsuit} = \frac{2\pi}{4} \int_{\partial\diamondsuit} \|\Delta\boldsymbol{\rho}_C\|^2 \left(\boldsymbol{\rho} \cdot \mathbf{b}\right) n_{\Delta\boldsymbol{\rho}_C}\, \mathrm{d}s - \frac{2\pi}{20} \left[\int_{\partial\diamondsuit} \|\Delta\boldsymbol{\rho}_C\|^2 \Delta\boldsymbol{\rho}_C\, n_{\Delta\boldsymbol{\rho}_C}\, \mathrm{d}s \right] \cdot \mathbf{b} = 2\pi \left[\frac{R^4}{4} \left(\boldsymbol{\rho}_C \cdot \mathbf{b}\right) (\beta - \alpha) + \frac{R^5}{5} \mathbf{N}^{(1)}_{\theta\diamondsuit} \cdot \mathbf{b} \right], \tag{68}$$

where use has been made of the identity (E.6) for $k = 1$ and the vector $\mathbf{N}^{(1)}_{\theta\diamondsuit}$ is provided in Eq. (D.1).

By invoking first Eq. (F.5) and then Eq. (E.6) for $k = 2$, it turns out to be

$$\begin{aligned}
\mathbf{J}^{(1),\mathrm{qua}}_{\mathrm{ax}\diamondsuit} &= \frac{2\pi}{5} \int_{\partial\diamondsuit} \|\Delta\boldsymbol{\rho}_C\|^2 \left(\boldsymbol{\rho} \cdot \mathbf{b}\right) \Delta\boldsymbol{\rho}_C\, n_{\Delta\boldsymbol{\rho}_C}\, \mathrm{d}s + 2\pi \int_{\diamondsuit} \|\Delta\boldsymbol{\rho}_C\|^2 \left(\boldsymbol{\rho} \cdot \mathbf{b}\right) \mathrm{d}A\, \boldsymbol{\rho}_C - \frac{\pi}{15} \left[\int_{\partial\diamondsuit} \|\Delta\boldsymbol{\rho}_C\|^2 \left[\otimes \Delta\boldsymbol{\rho}_C,\, 2\right] n_{\Delta\boldsymbol{\rho}_C}\, \mathrm{d}s \right] \mathbf{b} = \\
&= 2\pi \left[\frac{R^5}{5} \left(\boldsymbol{\rho}_C \cdot \mathbf{b}\right) \mathbf{N}^{(1)}_{\theta\diamondsuit} + \frac{R^6}{6} \mathbf{N}^{(2)}_{\theta\diamondsuit} \mathbf{b} \right] + \mathbf{J}^{(0),\mathrm{qua}}_{\mathrm{ax}\diamondsuit} \boldsymbol{\rho}_C,
\end{aligned} \tag{69}$$

in which $\mathbf{N}^{(1)}_{\theta\diamondsuit}$ and $\mathbf{N}^{(2)}_{\theta\diamondsuit}$ are supplied in Eqs. (D.1) and (D.2), respectively, while $\mathbf{J}^{(0),\mathrm{qua}}_{\mathrm{ax}\diamondsuit}$ is evaluated in Eq. (68).

Table 1
Algebraic formulas for computing mass moments of 2D domains and axisymmetric solids having density distributions (8)-(10).

Density distributions	2D domains		Axisymmetric solids	
	Polygons	Circular sectors	Polygons	Circular sectors
Polynomial	(24), (26) and (28)	-	(39), (41) and (43)	-
Exponential	(30), (32) and (34)	-	(44), (45) and (46)	-
Polynomial quadratic	(36)	-	(47)	-
Radially linear	-	(56), (57) and (59)	-	(65), (66) and (67)
Radially quadratic	-	(61), (62) and (63)	-	(68), (69) and (70)

Finally, it follows from Eq. (F.6) that

$$\begin{aligned}\mathbf{J}^{(2),\mathrm{qua}}_{\mathrm{ax}\diamondsuit} &= \frac{2\pi}{6}\int_{\partial\diamondsuit}\|\Delta\rho_C\|^2\,(\boldsymbol{\rho}\cdot\mathbf{b})\,\left[\otimes\Delta\rho_C,\,2\right]\,n_{\Delta\rho_C}\,\mathrm{d}s-\frac{2\pi}{42}\left[\int_{\partial\diamondsuit}\|\Delta\rho_C\|^2\,\left[\otimes\Delta\rho_C,\,3\right]\,n_{\Delta\rho_C}\,\mathrm{d}s\right]\mathbf{b}\\ &+\mathbf{J}^{(1),\mathrm{qua}}_{\mathrm{ax}\diamondsuit}\otimes\rho_C+\rho_C\otimes\mathbf{J}^{(1),\mathrm{qua}}_{\mathrm{ax}\diamondsuit}-\mathbf{J}^{(0),\mathrm{qua}}_{\mathrm{ax}\diamondsuit}\,\left(\rho_C\otimes\rho_C\right)=\\ &=2\pi\left[\frac{R^6}{6}\,(\rho_C\cdot\mathbf{b})\,\mathbf{N}^{(2)}_{\theta\diamondsuit}+\frac{R^7}{7}\,\mathbf{N}^{(3)}_{\theta\diamondsuit}\,\mathbf{b}\right]+\mathbf{J}^{(1),\mathrm{qua}}_{\mathrm{ax}\diamondsuit}\otimes\rho_C+\rho_C\otimes\mathbf{J}^{(1),\mathrm{qua}}_{\mathrm{ax}\diamondsuit}-\mathbf{J}^{(0),\mathrm{qua}}_{\mathrm{ax}\diamondsuit}\,\left(\rho_C\otimes\rho_C\right),\end{aligned}\tag{70}$$

where the expression of $\mathbf{N}^{(2)}_{\theta\diamondsuit}$ can be found in Eq. (D.2), that of $\mathbf{N}^{(3)}_{\theta\diamondsuit}$ in Eq. (D.3), while $\mathbf{J}^{(0),\mathrm{qua}}_{\mathrm{ax}\diamondsuit}$ and $\mathbf{J}^{(1),\mathrm{qua}}_{\mathrm{ax}\diamondsuit}$ are given by formulas (68) and (69), respectively.

9. Numerical applications

The formulas presented in the previous sections are verified both analytically and numerically by considering examples taken from [11,12] and additional ones proposed by the authors autonomously.

Specifically, denoting by $(\cdot)_{\mathrm{anl}}$ and $(\cdot)_{\mathrm{num}}$ the analytical and numerical evaluations of the three mass moments, we compute the quantities

$$\epsilon^{(k)}=\frac{\|\mathbf{J}^{(k)}_{\mathrm{anl}}-\mathbf{J}^{(k)}_{\mathrm{num}}\|}{\|\mathbf{J}^{(k)}_{\mathrm{anl}}\|},\tag{71}$$

to establish accuracy and reliability of the proposed formulas.

For readers comfort references to the formulas derived in the paper are summarised in Table 1.

9.1. Abat-jour domain

Let us consider a domain having the abat-jour shape shown in Fig. 3. The cross-section containing the axis of symmetry is composed of a quarter circle ($\diamondsuit$) and L-shaped polygon ($\mathbb{L}$); we assume

$$\varrho(\boldsymbol{\rho})=\begin{cases}e^{\alpha\,(\boldsymbol{\rho}\cdot\mathbf{e}_2)} & \text{if } \boldsymbol{\rho}\in\mathbb{L},\\ \|\boldsymbol{\rho}-\rho_C\|^2 & \text{if } \boldsymbol{\rho}\in\diamondsuit,\end{cases}$$

where $\alpha=1/10$ and $[\mathbf{e}_2]=[0,1]^T$.

Notice that the density varies along a direction $\mathbf{a}=\mathbf{e}_2$ different from that orthogonal to the axis of rotation, i.e. $\mathbf{b}=\mathbf{e}_1$.

Hence, the mass moments can be expressed as:

$$\begin{aligned}\frac{\mathbf{J}^{(0),\mathrm{exp}}_{\mathrm{ax}\Omega}+\mathbf{J}^{(0),\mathrm{qua}}_{\mathrm{ax}\diamondsuit}}{2\pi} &= \int_{\mathbb{L}} e^{\alpha\,(\boldsymbol{\rho}\cdot\mathbf{e}_2)}\,\left(\boldsymbol{\rho}\cdot\mathbf{e}_1\right)\,\mathrm{d}A+\int_{\diamondsuit}\|\boldsymbol{\rho}-\rho_C\|^2\,\left(\boldsymbol{\rho}\cdot\mathbf{e}_1\right)\,\mathrm{d}A,\\ \frac{\mathbf{J}^{(1),\mathrm{exp}}_{\mathrm{ax}\Omega}+\mathbf{J}^{(1),\mathrm{qua}}_{\mathrm{ax}\diamondsuit}}{2\pi} &= \int_{\mathbb{L}} e^{\alpha\,(\boldsymbol{\rho}\cdot\mathbf{e}_2)}\,\left(\boldsymbol{\rho}\cdot\mathbf{e}_1\right)\,\boldsymbol{\rho}\,\mathrm{d}A+\int_{\diamondsuit}\|\boldsymbol{\rho}-\rho_C\|^2\,\left(\boldsymbol{\rho}\cdot\mathbf{e}_1\right)\,\boldsymbol{\rho}\,\mathrm{d}A,\\ \frac{\mathbf{J}^{(2),\mathrm{exp}}_{\mathrm{ax}\Omega}+\mathbf{J}^{(2),\mathrm{qua}}_{\mathrm{ax}\diamondsuit}}{2\pi} &= \int_{\mathbb{L}} e^{\alpha\,(\boldsymbol{\rho}\cdot\mathbf{e}_2)}\,\left(\boldsymbol{\rho}\cdot\mathbf{e}_1\right)\,(\boldsymbol{\rho}\otimes\boldsymbol{\rho})\,\mathrm{d}A+\int_{\diamondsuit}\|\boldsymbol{\rho}-\rho_C\|^2\,\left(\boldsymbol{\rho}\cdot\mathbf{e}_1\right)\,(\boldsymbol{\rho}\otimes\boldsymbol{\rho})\,\mathrm{d}A.\end{aligned}$$

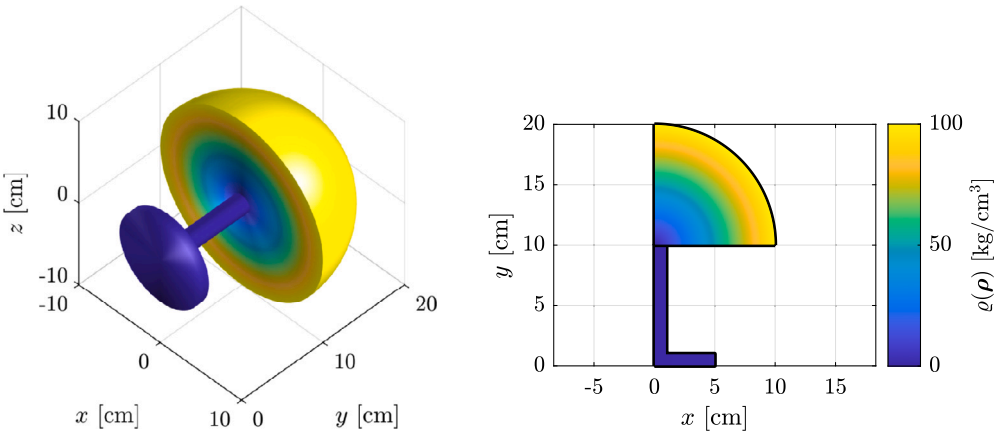

(a) *3D plot*

(b) *Density distribution in a plane containing the axis of symmetry*

Fig. 3. Abat-jour domain and its density distributions having laws specified in Eqs. (9) and (50).

The previous integrals over the L-polygon [quarter circle] can be computed by using Eqs. (19) [(68), (69) and (70)]. The analytical evaluation of the three mass moments is given by

$$[\mathbf{J}^{(0),\mathrm{exp}}_{\mathrm{ax}\Omega} + \mathbf{J}^{(0),\mathrm{qua}}_{\mathrm{ax}\diamondsuit}]_{\mathrm{anl}} = 10\,\pi\left(3975 + 24\,\sqrt[10]{e} + e\right),$$

$$[\mathbf{J}^{(1),\mathrm{exp}}_{\mathrm{ax}\Omega} + \mathbf{J}^{(1),\mathrm{qua}}_{\mathrm{ax}\diamondsuit}]_{\mathrm{anl}} = \pi\begin{bmatrix} \frac{20}{3}\left(-125 + 124\,\sqrt[10]{e} + e + 12\,500\,\pi\right) \\ \frac{20}{3}\left(85\,375 - 324\,\sqrt[10]{e}\right) \end{bmatrix},$$

$$[\mathbf{J}^{(2),\mathrm{exp}}_{\mathrm{ax}\Omega} + \mathbf{J}^{(2),\mathrm{qua}}_{\mathrm{ax}\diamondsuit}]_{\mathrm{anl}} = \pi\begin{bmatrix} \frac{5}{21}\left(21\left(624\,\sqrt[10]{e} + e\right) + 7\,986\,875\right) & J_{12} \\ J_{21} & \frac{40}{7}\left(1\,441\,250 + 7602\,\sqrt[10]{e} + 175\,e\right) \end{bmatrix},$$

$$J_{12} = J_{21} = \frac{40}{21}\left(625\,(807 + 700\,\pi) - 3906\,\sqrt[10]{e}\right),$$

providing the following relative errors:

$$\epsilon^{(0)} = 0,$$

$$\epsilon^{(1)} \approx 2.4471 \times 10^{-16},$$

$$\epsilon^{(2)} \approx 2.3994 \times 10^{-16}.$$

The results obtained do agree with the analytical evaluation of the mass moments, except for the machine precision.

9.2. Torus with a rounded square annulus cross-section

Let us consider the torus having the rounded square annulus cross-section depicted in Fig. 4. As it has been assumed in [12], the density distribution increases with a constant rate, from 1 kg/cm^3 on the inner side of the cross-section to 6 kg/cm^3 on the outer side, along the radial direction starting from the centre of gravity. Specifically, decomposing the rounded square annulus into

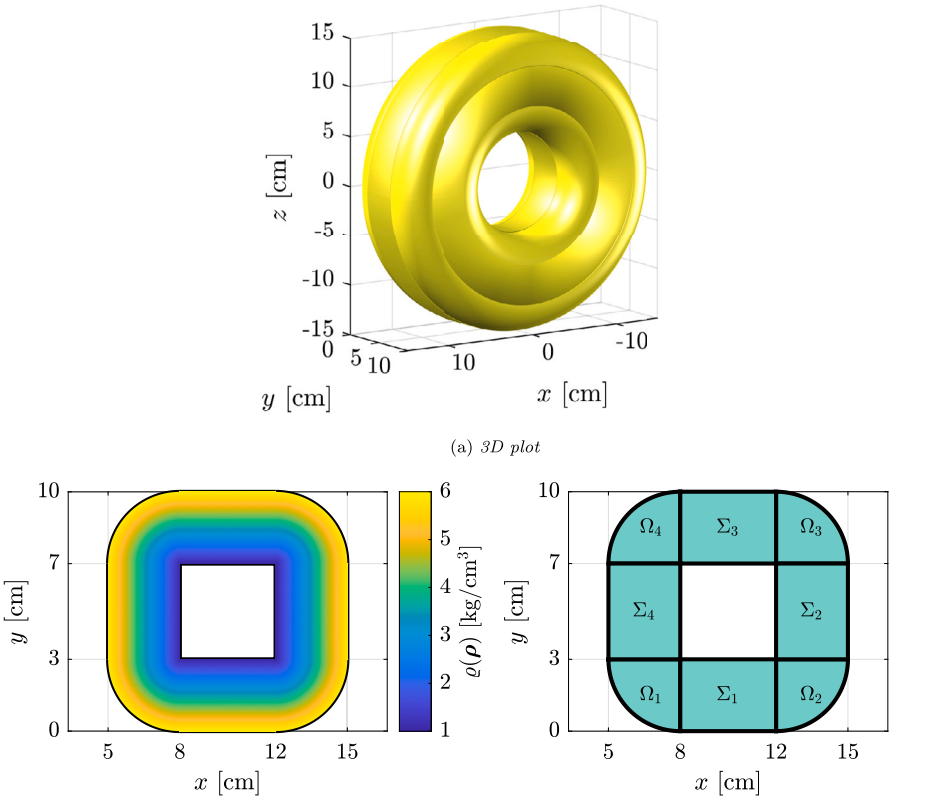

(a) *3D plot*

(b) *Density distribution in a plane containing the axis of symmetry*

(c) *Cross-section decomposition by subdomains*

Fig. 4. Torus with a rounded square annulus cross-section having linear density distribution.

subdomains, as illustrated in Fig. 4(c), one can write

$$\varrho(\boldsymbol{\rho}) = \begin{cases} 6 - \dfrac{5}{3}\left(\boldsymbol{\rho}\cdot\mathbf{e}_2\right) & \text{if } \boldsymbol{\rho}\in\Sigma_1, \\ -19 + \dfrac{5}{3}\left(\boldsymbol{\rho}\cdot\mathbf{e}_1\right) & \text{if } \boldsymbol{\rho}\in\Sigma_2, \\ -\dfrac{32}{3} + \dfrac{5}{3}\left(\boldsymbol{\rho}\cdot\mathbf{e}_2\right) & \text{if } \boldsymbol{\rho}\in\Sigma_3, \\ \dfrac{43}{3} - \dfrac{5}{3}\left(\boldsymbol{\rho}\cdot\mathbf{e}_1\right) & \text{if } \boldsymbol{\rho}\in\Sigma_4, \\ 1 + \dfrac{5}{R}\|\boldsymbol{\rho}-\boldsymbol{\rho}_{C_1}\| & \text{if } \boldsymbol{\rho}\in\Omega_1, \\ 1 + \dfrac{5}{R}\|\boldsymbol{\rho}-\boldsymbol{\rho}_{C_2}\| & \text{if } \boldsymbol{\rho}\in\Omega_2, \\ 1 + \dfrac{5}{R}\|\boldsymbol{\rho}-\boldsymbol{\rho}_{C_3}\| & \text{if } \boldsymbol{\rho}\in\Omega_3, \\ 1 + \dfrac{5}{R}\|\boldsymbol{\rho}-\boldsymbol{\rho}_{C_4}\| & \text{if } \boldsymbol{\rho}\in\Omega_4, \end{cases}$$

where $R = 3$, $[\boldsymbol{\rho}_{C_1}] = [8,3]^T$, $[\boldsymbol{\rho}_{C_2}] = [12,3]^T$, $[\boldsymbol{\rho}_{C_3}] = [12,7]^T$ and $[\boldsymbol{\rho}_{C_4}] = [8,7]^T$.

Hence, making reference to the subdomain Ω_1 as an example, the mass moments read as follows on account of formulas (18), (65), (66) and (67)

$$\frac{\mathbf{J}^{(0),\mathrm{lin}}_{\mathrm{ax}\diamond}}{2\pi} = \int_{\Omega_1} \boldsymbol{\rho}\,\mathrm{d}A\cdot\mathbf{e}_1 + \frac{5}{3}\int_{\Omega_1}\|\boldsymbol{\rho}-\boldsymbol{\rho}_C\|\,(\boldsymbol{\rho}\cdot\mathbf{e}_1)\,\mathrm{d}A = \mathbf{s}_\diamond\cdot\mathbf{e}_1 + \frac{5}{3}\int_{\Omega_1}\|\boldsymbol{\rho}-\boldsymbol{\rho}_C\|\,(\boldsymbol{\rho}\cdot\mathbf{e}_1)\,\mathrm{d}A,$$

$$\frac{\mathbf{J}^{(1),\mathrm{lin}}_{\mathrm{ax}\diamond}}{2\pi} = \left[\int_{\Omega_1}(\boldsymbol{\rho}\otimes\boldsymbol{\rho})\,\mathrm{d}A\right]\mathbf{e}_1 + \frac{5}{3}\int_{\Omega_1}\|\boldsymbol{\rho}-\boldsymbol{\rho}_C\|\,(\boldsymbol{\rho}\cdot\mathbf{e}_1)\,\boldsymbol{\rho}\,\mathrm{d}A = \mathbf{J}_\diamond\mathbf{e}_1 + \frac{5}{3}\int_{\Omega_1}\|\boldsymbol{\rho}-\boldsymbol{\rho}_C\|\,(\boldsymbol{\rho}\cdot\mathbf{e}_1)\,\boldsymbol{\rho}\,\mathrm{d}A,$$

$$\frac{\mathbf{J}^{(2),\mathrm{lin}}_{\mathrm{ax}\diamond}}{2\pi} = \left[\int_{\Omega_1}(\boldsymbol{\rho}\otimes\boldsymbol{\rho}\otimes\boldsymbol{\rho})\,\mathrm{d}A\right]\mathbf{e}_1 + \frac{5}{3}\int_{\Omega_1}\|\boldsymbol{\rho}-\boldsymbol{\rho}_C\|\,(\boldsymbol{\rho}\cdot\mathbf{e}_1)\,(\boldsymbol{\rho}\otimes\boldsymbol{\rho})\,\mathrm{d}A = \mathbf{J}^{(3)}_\diamond\mathbf{e}_1 + \frac{5}{3}\int_{\Omega_1}\|\boldsymbol{\rho}-\boldsymbol{\rho}_C\|\,(\boldsymbol{\rho}\cdot\mathbf{e}_1)\,(\boldsymbol{\rho}\otimes\boldsymbol{\rho})\,\mathrm{d}A,$$

where $\mathbf{s}_\diamond$ and $\mathbf{J}_\diamond$ have been computed in Eqs. (53) and (55), while $\mathbf{J}^{(3)}_\diamond$ is computed using Eq. (G.13) of the SM 7. For rectangular domains such as Σ_1 reference can be made to Eqs. (39), (41), and (43).

Analytical expressions for the mass moments with respect to the reference frame depicted in Fig. 4 are as follows:

$$[\mathbf{J}^{(0)}]_{\mathrm{anl}} = 60\,\pi(56+13\,\pi),$$

$$[\mathbf{J}^{(1)}]_{\mathrm{anl}} = \begin{bmatrix} \frac{1}{2}\pi(75592+16629\,\pi) \\ 300\,\pi(56+13\,\pi) \end{bmatrix},$$

$$[\mathbf{J}^{(2)}]_{\mathrm{anl}} = \begin{bmatrix} 15\,\pi\,(30792+6229\,\pi) & \frac{5}{2}\,\pi(75592+16629\,\pi) \\ \frac{5}{2}\,\pi(75592+16629\,\pi) & 5\,\pi(25192+4929\,\pi) \end{bmatrix},$$

and yield the following relative errors:

$$\epsilon^{(0)} = 0,$$

$$\epsilon^{(1)} = 0,$$

$$\epsilon^{(2)} \approx 1.8927\times10^{-16};$$

this confirms the accuracy of the formulas derived in the paper if compared with the results outlined in [12].

9.3. Longitudinal section of a human femure

As a final example, we consider the longitudinal section, obtained by a scan of a human femure, for which a functionally graded variation of density has been assumed with a direction tilt of forty-five degrees along the bone, as illustrated in Fig. 5(a); specifically, the mass density reads

$$\varrho(\boldsymbol{\rho}\cdot\mathbf{a}) = C_0 + C_1\,(\boldsymbol{\rho}\cdot\mathbf{a}),$$

where $[\mathbf{a}] = [1/\sqrt{2}, 1/\sqrt{2}]^T$, $C_0 = 13/(500\times10^3)$ [kg/cm^3] and $C_1 = 13/(500\times10^3)$ [kg/cm^4].

Recalling Eq. (13), the generalised mass moments are given by

$$\mathbf{J}^{(0),\mathrm{pln}}_{2\Omega} = C_0\,A + \frac{C_1}{2}\int_{\partial\Omega}(\boldsymbol{\rho}\cdot\mathbf{a})\,(\boldsymbol{\rho}\cdot\mathbf{n})\,\mathrm{d}s,$$

$$\mathbf{J}^{(1),\mathrm{pln}}_{2\Omega} = C_0\,\mathbf{s} + \frac{C_1}{3}\int_{\partial\Omega}(\boldsymbol{\rho}\cdot\mathbf{a})\,(\boldsymbol{\rho}\cdot\mathbf{n})\,\boldsymbol{\rho}\,\mathrm{d}s,$$

$$\mathbf{J}^{(2),\mathrm{pln}}_{2\Omega} = C_0\,\mathbf{J} + \frac{C_1}{4}\int_{\partial\Omega}(\boldsymbol{\rho}\cdot\mathbf{a})\,(\boldsymbol{\rho}\cdot\mathbf{n})\,(\boldsymbol{\rho}\otimes\boldsymbol{\rho})\,\mathrm{d}s,$$

where A, $\mathbf{s}$ and $\mathbf{J}$ are the mass moments associated with the femur supposed to be homogeneous. The geometry of the femur has been assigned by approximating its boundary by means of a polygon with sixty-one sides and the generalised mass moments have been computed by exploiting Eqs. (23), (25) and (27).

To make a comparison of the analytical results with the numerical ones, a finite element model of the femure has been considered by subdividing the longitudinal section of the femur into triangular elements, see, e.g., Fig. 5(b). The red dots visible in the figure represent the position of the Gauss points associated with a given order of the quadrature rule. Needless to say, the number of triangular elements and the order of quadrature have direct consequence on the accuracy of the solution and computing time, especially in nonlinear analyses in which meshing of the domain needs to be continuously updated due to changes of the geometry.

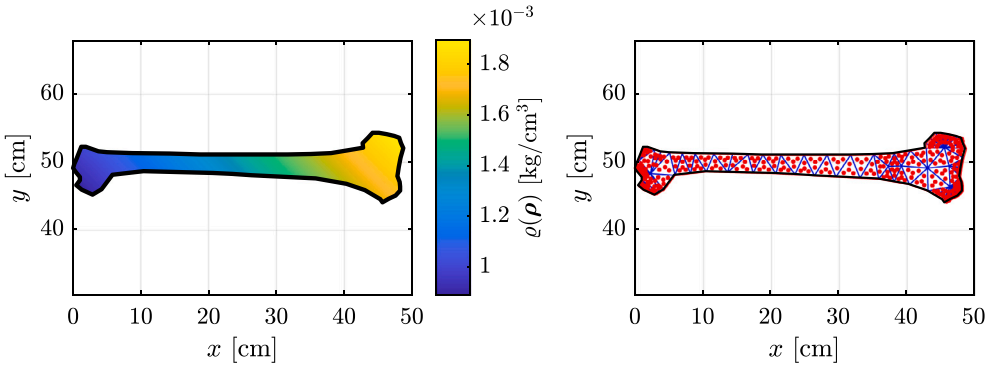

(a) *Density distribution* (b) *Domain discretisation and location of Gauss points*

Fig. 5. Longitudinal section of a human femure having a linear density distribution.

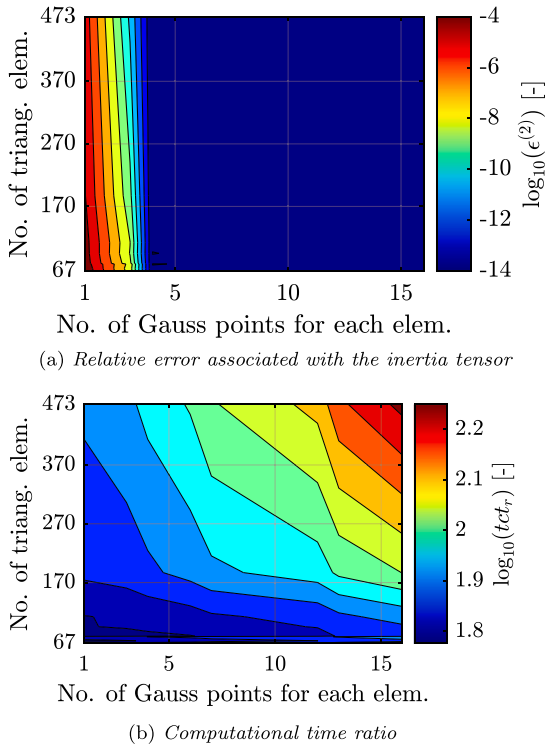

(a) *Relative error associated with the inertia tensor*

(b) *Computational time ratio*

Fig. 6. Contour maps in logarithmic scale of the relative error for the inertia tensor (a) and computational time ratio (b), as a function of the number of triangular elements and Gauss points.

To ascertain the accuracy and computational demand of the proposed approach with respect to a numerical one we have computed the relative error $\epsilon^{(2)}$ defined in (71) for the inertia tensor and evaluated the total computational time ratio (tct_r) associated with the proposed formulation (*PF*) and Gauss quadrature (*GQ*)

$$tct_r = \frac{tct_{GQ}}{tct_{PF}}.$$

The quantities $\epsilon^{(2)}$ and tct_r are plotted in Fig. 6(a) and (b), respectively, against the number of triangular elements and Gauss points for each element.

The warmer colours in Fig. 6(a) indicate regions where $\epsilon^{(2)}$ reaches its maximum value, signifying the least accuracy in evaluating the inertia tensor. To achieve a value of $\epsilon^{(2)}$ for the inertia tensor obtained numerically, $\epsilon^{(2)}_{\text{num}} = 1.0610 \times 10^{-14}$, comparable to that obtained with the analytical formulas, whose order of magnitude is 10^{-16}, a minimum of sixty-seven triangular elements is required to discretise the human femur, using four Gauss points for each triangular element.

However, considering that $tct_{PF} \approx 0.0019$ seconds, it becomes apparent from Fig. 6(b) that the Gauss quadrature method is notably slower than the proposed formulas. This difference amounts to at least two orders of magnitude, assuming a minimum requirement of sixty-seven triangular elements with four Gauss points per element to discretise the human femur. The outcomes remain largely the same even if one opts for a reduced number of triangular elements and a single Gauss point, albeit at the cost of a reduced accuracy in computing mass moments.

Please notice that the analyses have been run on a computer having an AMD Ryzen™ 3 3250U processor and CPU at 2.60 GHz with 8 GB of RAM.

10. Conclusions

The mass moments of functionally graded 2D domains and axisymmetric solids endowed with polynomial and exponential density distributions have been computed analytically by means of algebraic formulas in case of polygonal domains and circular sectors. Besides the coefficients defining the density variation, the formulas derived in the paper are expressed as a function of the coordinates of the vertices that define the polygonal domains while, for circular sectors, as a function of the anomalies of the segments defining the sector and the coordinates of the relevant endpoints.

Numerical examples, including cases sourced from [11,12] as well as some others specifically devised by the authors, have been used to validate the generality, accuracy and computational efficiency of the proposed formulation with respect to those based upon integral equations [11,12], that require the solution of a linear system of equations, the finite element method or the use of a Monte Carlo technique [37].

In particular, the longitudinal section of a human femure, having a complex geometry and made of functionally graded material exhibiting a linear density distribution, has been used to compare the overall efficiency of the proposed approach, in terms of accuracy and computational time, with respect to that entailed by the finite element method.

It has been shown that at least sixty-seven triangular elements and four Gauss points per element are required to achieve an accuracy comparable to that of the analytical formulas, although the computational time increased by two orders of magnitude.

Actually, the computational time required by the proposed approach basically depends on the number of points used to approximate the boundary of the domain by a polygon, while, even neglecting the time required to mesh the domain, that required by the finite element method depends upon the number of elements used to discretise the domain and the quadrature rule adopted for each element. In particular, the number of elements do significantly increase for domains characterised by larger aspect ratios, what makes the proposed approach even more convenient for the applications since only the boundary of the domain needs to be considered.

Time savings entailed by the analytical formulas obtained in the paper become even greater for nonlinear structural analyses since, at each iteration, it is required an updating of the mass moments associated with changes in the geometric or material properties of the domain.

Hence, the methodology illustrated in the paper is characterised by simplicity, straightforward implementation and applicability to objects made of functionally graded materials such as those produced by modern 3D printing technology and widely used in aerospace, automobile, biomedical and defence areas. For instance, modelling the behaviour of functionally graded beams and solids, for which variations in the Young modulus are assumed [34–36,38], does not require a new computational scheme for integral expressions of the generalised stiffness matrices.

The application of the proposed approach to functionally graded beams and to three-dimensional solids endowed with further density distributions will be addressed in forthcoming papers.

CRediT authorship contribution statement

Davide Pellecchia: Conceptualisation, Methodology, Software, Validation, Writing – original draft, Writing – review & editing. **Nicolò Vaiana:** Methodology, Validation. **Salvatore Sessa:** Validation, Supervision. **Anna Castellano:** Conceptualisation, Methodology.

Declaration of competing interest

The authors declare that they have no known competing financial interests or personal relationships that could have appeared to influence the work reported in this paper.

Data availability

Data will be made available on request.

Acknowledgements

The authors are grateful to the reviewers for their useful suggestions and particularly indebted to the Associate Editor for his continuous support in the organisation of the paper and constructive criticism of the earlier versions of the manuscript. Initial interest for the subject of the manuscript and subsequent proofreading by Prof. Lina Mallozzi, University of Naples Federico II, is also gratefully acknowledged.

Appendix A. Supplementary material

Supplementary material related to this article can be found online at https://doi.org/10.1016/j.apm.2024.01.028.

References

[1] A.O. Ghaziani, R. Soheilifard, S. Kowsar, The effect of functionally graded materials on bone remodeling around osseointegrated trans-femoral prostheses, J. Mech. Behav. Biomed. Mater. 118 (2021) 104426.
[2] Y. Wang, Y. Zhou, C. Feng, J. Yang, et al., Numerical analysis on stability of functionally graded graphene platelets (gpls) reinforced dielectric composite plate, Appl. Math. Model. 101 (2022) 239–258, https://doi.org/10.1016/j.apm.2021.08.003.
[3] J.K. Lee, B.K. Lee, Free vibration and buckling of tapered columns made of axially functionally graded materials, Appl. Math. Model. 75 (2019) 73–87, https://doi.org/10.1016/j.apm.2019.05.010.
[4] Q. Song, J. Shi, Z. Liu, Vibration analysis of functionally graded plate with a moving mass, Appl. Math. Model. 46 (2017) 141–160, https://doi.org/10.1016/j.apm.2017.01.073.
[5] R.A. Diaz, W.J. Herrera, R. Martinez, Moments of inertia for solids of revolution and variational methods, Eur. J. Phys. 27 (2) (2006) 183, https://doi.org/10.1088/0143-0807/27/2/001.
[6] W. Lacarbonara, Nonlinear Structural Mechanics. Theory, Dynamical Phenomena and Modeling, Springer, New York, NY, 2013.
[7] M. Paradiso, F. Marmo, L. Rosati, Consistent derivation of a beam model from the Saint Venant's solid model, Int. J. Solids Struct. 159 (2019) 90–110, https://doi.org/10.1016/j.ijsolstr.2018.09.021.
[8] M. Paradiso, N. Vaiana, S. Sessa, F. Marmo, et al., A BEM approach to the evaluation of warping functions in the Saint Venant theory, Eng. Anal. Bound. Elem. 113 (2020) 359–371, https://doi.org/10.1016/j.enganabound.2020.01.004.
[9] D. Pellecchia, S. Lo Feudo, N. Vaiana, J.-L. Dion, et al., A procedure to model and design elastomeric-based isolation systems for the seismic protection of rocking art objects, Comput.-Aided Civ. Infrastruct. Eng. 37 (10) (2022) 1298–1315, https://doi.org/10.1111/mice.12775.
[10] R. Ceravolo, M.L. Pecorelli, L. Zanotti Fragonara, Semi-active control of the rocking motion of monolithic art objects, J. Sound Vib. 374 (2016) 1–16, https://doi.org/10.1016/j.jsv.2016.03.038.
[11] Y. Ochiai, Numerical integration to obtain moment of inertia of nonhomogeneous material, Eng. Anal. Bound. Elem. 101 (2019) 149–155, https://doi.org/10.1016/j.enganabound.2019.01.001.
[12] Y. Ochiai, Numerical integration to obtain second moment of inertia of axisymmetric heterogeneous body, Eng. Anal. Bound. Elem. 133 (2021) 398–406, https://doi.org/10.1016/j.enganabound.2021.09.016.
[13] C. Brebbia, J. Telles, L. Wrobel, Boundary Element Techniques: Theory and Applications in Engineering, Springer, Berlin, Heidelberg, 1984.
[14] G. Romano, Scienza delle Costruzioni, vol. 2 (in Italian), Hevelius, 2003.
[15] W. Yeih, J. Chang, J. Chen, A boundary formulation for calculating moments of an arbitrary closed planar region, Eng. Anal. Bound. Elem. 23 (7) (1999) 611–617, https://doi.org/10.1016/S0955-7997(99)00004-1.
[16] F. Marmo, L. Rosati, The fiber-free approach in the evaluation of the tangent stiffness matrix for elastoplastic uniaxial constitutive laws, Int. J. Numer. Methods Eng. 94 (9) (2013) 868–894, https://doi.org/10.1002/nme.4484.
[17] G. Alfano, F. Marmo, L. Rosati, An unconditionally convergent algorithm for the evaluation of the ultimate limit state of rc sections subject to axial force and biaxial bending, Int. J. Numer. Methods Eng. 72 (8) (2007) 924–963, https://doi.org/10.1002/nme.2033.
[18] F. Marmo, R. Serpieri, L. Rosati, Ultimate strength analysis of prestressed reinforced concrete sections under axial force and biaxial bending, Comput. Struct. 89 (1) (2011) 91–108, https://doi.org/10.1016/j.compstruc.2010.08.005.
[19] S. Sessa, F. Marmo, N. Vaiana, L. Rosati, Probabilistic assessment of axial force–biaxial bending capacity domains of reinforced concrete sections, Meccanica 54 (9) (2019) 1451–1469, https://doi.org/10.1007/s11012-019-00979-4.
[20] L. Rosati, F. Marmo, Closed-form expressions of the thermo-mechanical fields induced by a uniform heat source acting over an isotropic half-space, Int. J. Heat Mass Transf. 75 (2014) 272–283, https://doi.org/10.1016/j.ijheatmasstransfer.2014.03.069.
[21] M.G. D'Urso, F. Marmo, Vertical stress distribution in isotropic half-spaces due to surface vertical loadings acting over polygonal domains, Z. Angew. Math. Mech. 95 (1) (2015) 91–110, https://doi.org/10.1002/zamm.201300034.
[22] F. Marmo, L. Rosati, A general approach to the solution of Boussinesq's problem for polynomial pressures acting over polygonal domains, J. Elast. 122 (1) (2016) 75–112, https://doi.org/10.1007/s10659-015-9534-5.
[23] F. Marmo, S. Sessa, L. Rosati, Analytical solution of the Cerruti problem under linearly distributed horizontal loads over polygonal domains, J. Elast. 124 (1) (2016) 27–56, https://doi.org/10.1007/s10659-015-9560-3.
[24] R. Fosdick, P. Foti, A. Fraddosio, S. Marzano, Shear driven planar Couette and Taylor-like instabilities for a class of compressible isotropic elastic solids, Z. Angew. Math. Phys. 61 (3) (2010) 537–554, https://doi.org/10.1007/s00033-009-0020-4.
[25] R. Fosdick, P. Foti, A. Fraddosio, M.D. Piccioni, A lower bound estimate of the critical load for compressible elastic solids, Contin. Mech. Thermodyn. 22 (2) (2010) 77–97, https://doi.org/10.1007/s00161-009-0133-1.
[26] R. Fosdick, P. Foti, A. Fraddosio, S. Marzano, et al., Taylor-like bifurcations for a compressible isotropic elastic tube, Math. Mech. Solids 19 (8) (2014) 966–987, https://doi.org/10.1177/1081286513496576.
[27] R. Fosdick, P. Foti, A. Fraddosio, S. Marzano, M.D. Piccioni, A lower bound estimate of the critical load in bifurcation analysis for incompressible elastic solids, Math. Mech. Solids 20 (1) (2015) 53–79, https://doi.org/10.1177/1081286514543599.
[28] M.G. D'Urso, S. Trotta, Comparative assessment of linear and bilinear prism-based strategies for terrain correction computations, J. Geod. 89 (3) (2015) 199–215, https://doi.org/10.1007/s00190-014-0770-4.
[29] M.G. D'Urso, A remark on the computation of the gravitational potential of masses with linearly varying density, in: N. Sneeuw, P. Novák, M. Crespi, F. Sansò (Eds.), VIII Hotine-Marussi Symposium on Mathematical Geodesy, Springer International Publishing, 2016, pp. 205–212.
[30] S. De Cicco, D. Iesan, Thermal effects in anisotropic porous elastic rods, J. Therm. Stresses 36 (2022) 364–377, https://doi.org/10.1080/01495739.2013.770696.
[31] S. De Cicco, Non simple elastic materials with double porosity structure, Arch. Mech. 74 (2–3) (2022) 127–142, https://doi.org/10.24423/aom.4003.
[32] S. Trotta, F. Marmo, L. Rosati, Analytical expression of the Eshelby tensor for arbitrary polygonal inclusions in two-dimensional elasticity, Composites, Part B, Eng. 106 (2016) 48–58, https://doi.org/10.1016/j.compositesb.2016.09.010.
[33] S. Trotta, G. Zuccaro, S. Sessa, F. Marmo, et al., On the evaluation of the Eshelby tensor for polyhedral inclusions of arbitrary shape, Composites, Part B, Eng. 144 (2018) 267–281, https://doi.org/10.1016/j.compositesb.2018.01.012.
[34] E. Ruocco, J. Reddy, A closed-form solution for accurate stress analysis of functionally graded Reddy beams, Compos. Struct. 307 (2023) 116676, https://doi.org/10.1016/j.compstruct.2023.116676.
[35] W. Peng, T. He, Elastoplastic nonlinear analysis of functionally graded beams utilizing the symplectic method, Arch. Appl. Mech. 91 (12) (2021) 4735–4750, https://doi.org/10.1007/s00419-021-02030-z.
[36] J. Reddy, P. Nampally, A.R. Srinivasa, Nonlinear analysis of functionally graded beams using the dual mesh finite domain method and the finite element method, Int. J. Non-Linear Mech. 127 (2020) 103575, https://doi.org/10.1016/j.ijnonlinmec.2020.103575.

[37] R.E. Caflisch, Monte Carlo and quasi-Monte Carlo methods, Acta Numer. 7 (1998) 1–49, https://doi.org/10.1017/S0962492900002804.
[38] Y. Li, Z. Feng, L. Hao, L. Huang, et al., A review on functionally graded materials and structures via additive manufacturing: from multi-scale design to versatile functional properties, Adv. Mater. Technol. 5 (6) (2020) 1900981, https://doi.org/10.1002/admt.201900981.